Chiral magnetic effect & anomalous transport from real-time lattice simulations

Soeren Schlichting

Mark Mace, SS, Raju Venugopalan PRD93 (2016) no.7, 074036

Niklas Mueller, SS, Sayantan Sharma arXiv:1606.00342

Mark Mace,Niklas Mueller, SS, Sayantan Sharma in preparation

BROOKHAVEN
NATIONAL LABORATORY

Outline

Introduction & Motivation

Sphaleron transitions and generation of axial charge imbalance out of equilibrium

Chiral magnetic effect & anomalous transport from real-time lattice simulations

Chiral magnetic effect

Discovery of new kind of conductivity for systems with chiral fermions and chirality imbalanced

(Fukushima, Kharzeev, Warringa PRD 78 (2008) 074033)

$$\vec{j}_V \propto n_5 \vec{B}$$

n_5: axial charge imbalance

B: magnetic field

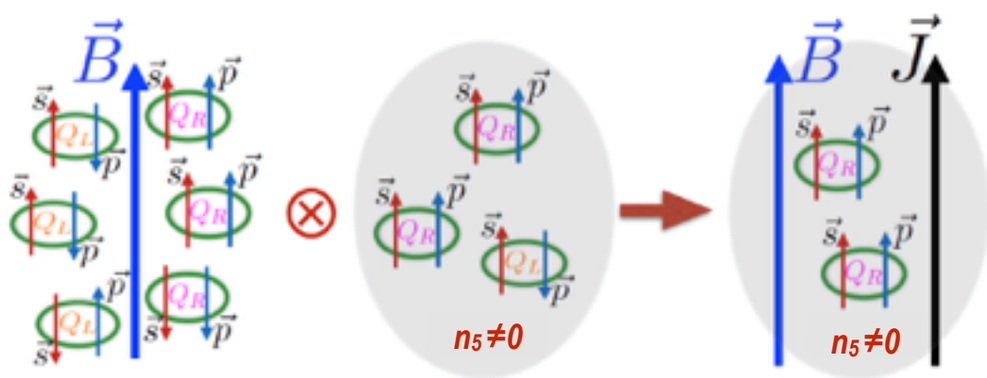

Kharzeev, Liao, Voloshin, Wang
Prog. Part. Nucl. Phys. 88 (2016) 1-28

Several possible manifestations of this effect from high-energy QCD to Dirac/Weyl semi-metals

Observation in $ZrTe_5$: Kharzeev et al. Nature Physics (2016)

CME in Heavy-Ion collisions

Magnetic field: Spectators in off-central collisions create a strong magnetic field eB ~ m_π^2 (unit conversion $m_\pi^2 \sim 10^{14}$ T)

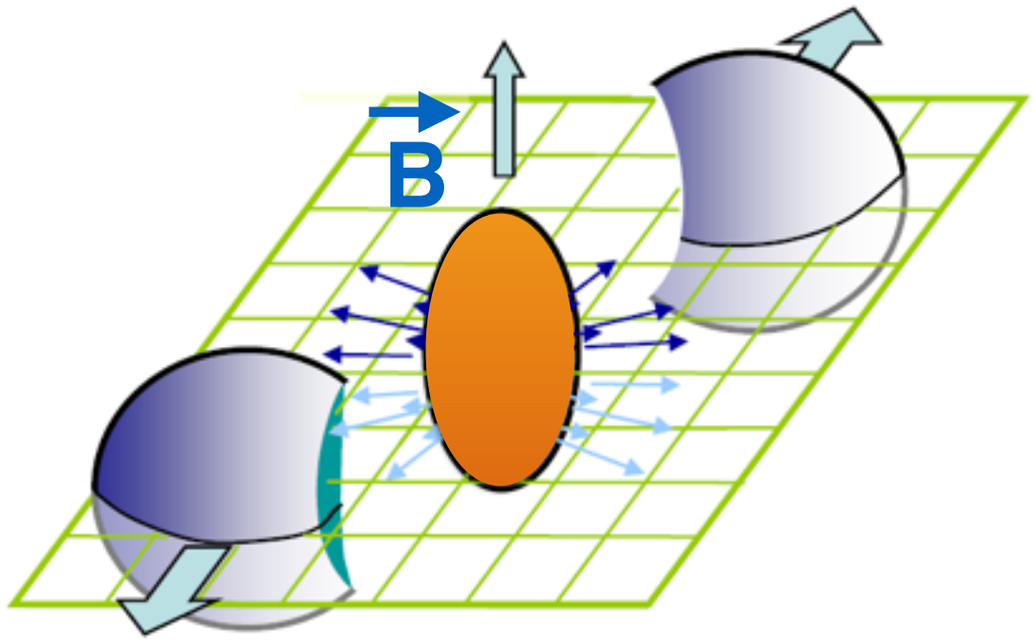

STAR PRC 81 (2010) 054908

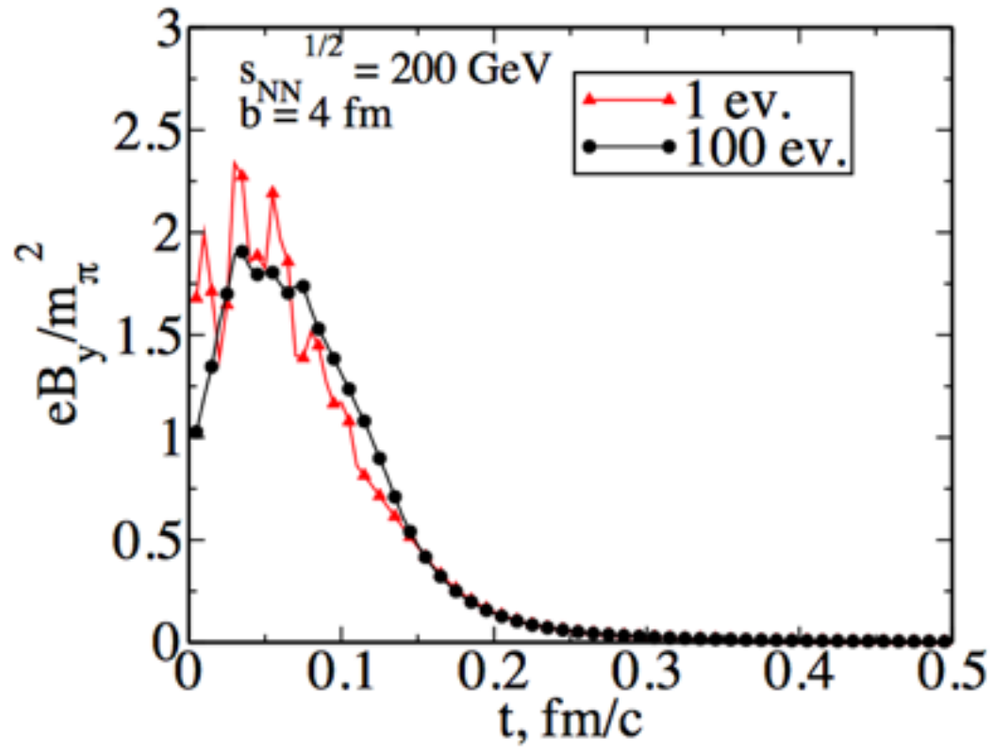

Skokov,Illarionov,Toneev
Int.J.Mod.Phys. A24 (2009) 5925-5932

Expected life-time of magnetic field is short < 1 fm/c, so the effect should take place during the pre-equilibrium stage

CME in Heavy-Ion collisions

Axial charge imbalance (n_5): Sourced by fluctuations of the non-abelian field strength tensor due to the axial anomaly

$$\partial_\mu j^\mu_{5,f} = 2m_f \bar{q}\gamma_5 q - \frac{g^2}{16\pi^2} F^a_{\mu\nu}\tilde{F}^{\mu\nu}_a$$

axial current $j^\mu_5 = (n_5, \vec{j}_5)$

quark mass

field-strength fluctuations $\propto \vec{E}\cdot\vec{B}$

$\vec{E}\cdot\vec{B}$

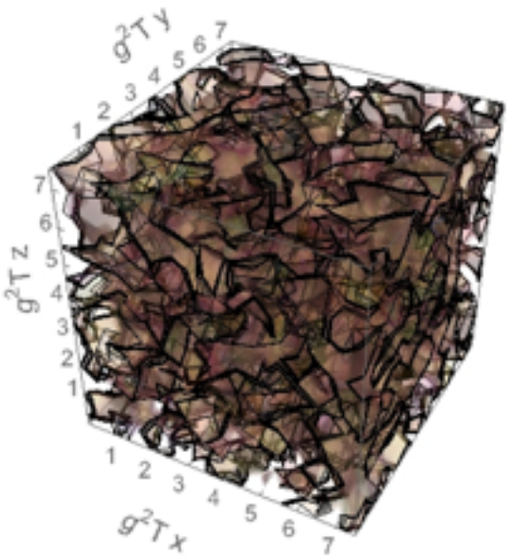

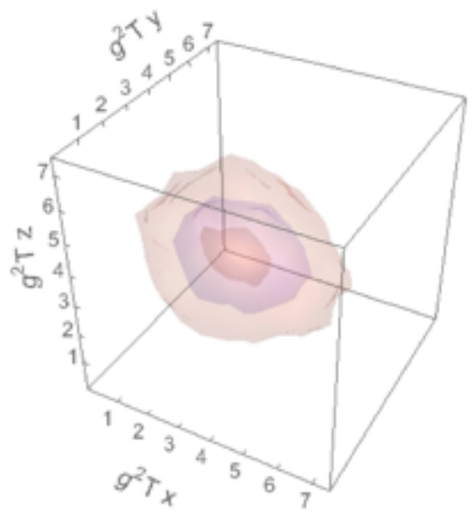

Considering the contribution to local imbalances of the axial charge $n_5(x,t)$ one can distinguish contributions due to

- space-time dependent fluctuations of $\vec{E}\cdot\vec{B}$
- topological sphaleron transitions

Naturally expect local fluctuations of axial charge density in each event

CME in Heavy-Ion collisions

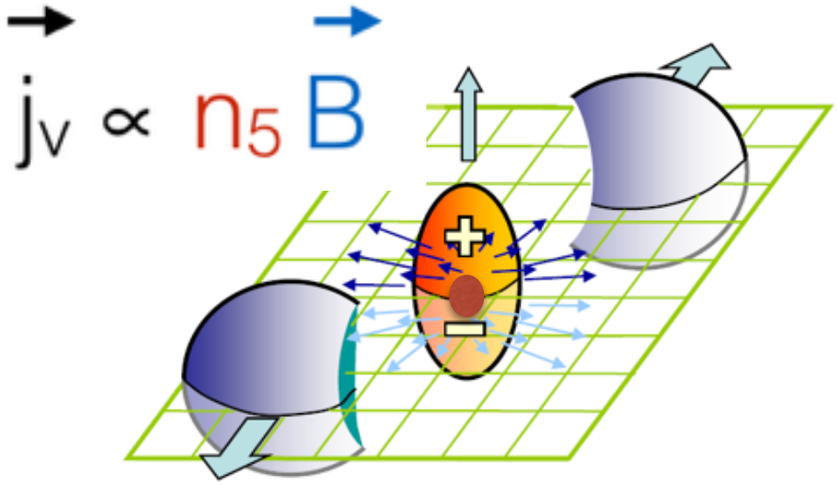

Experimental status:

Since axial charge fluctuates from event to event on average $\langle j_V \rangle = 0$, so one can only measure fluctuations

Basic idea is to look for back-to-back correlations of opposite charge particles with respect to the reaction plane

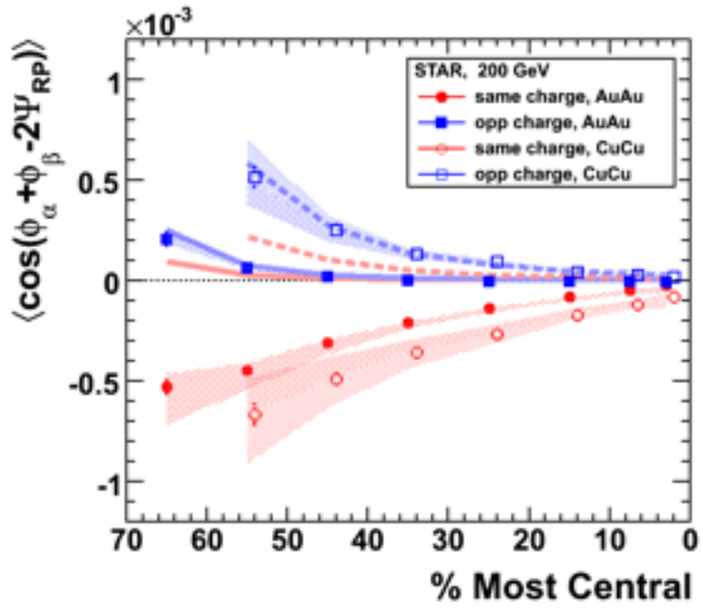

STAR PRC 81 (2010) 054908

While intriguing hints of CME and associated phenomena have been observed at RHIC and LHC, measurements are also subject to potentially large backgrounds

``Chiral Magnetic Effect Task Force Report,'' arXiv:1608.00982 [nucl-th]

Isobar scan envisioned as decisive test to isolate signal vs. background

Challenges with regard to CME in heavy-ion collisions

Quantitative theoretical understanding of anomaly induced transport phenomena (CME,CMW,…) in heavy-ion collisions important experimental searches for these effects

Since life time of magnetic field is presumably very short (~0.1-1 fm/c) system is out-of-equilibrium during the time scales relevant for CME & Co.

Need to understand generation of axial charge imbalance under non-equilibrium conditions

Study the real-time dynamics of fermions in out-of-equilibrium plasma in the presence of a magnetic field

2

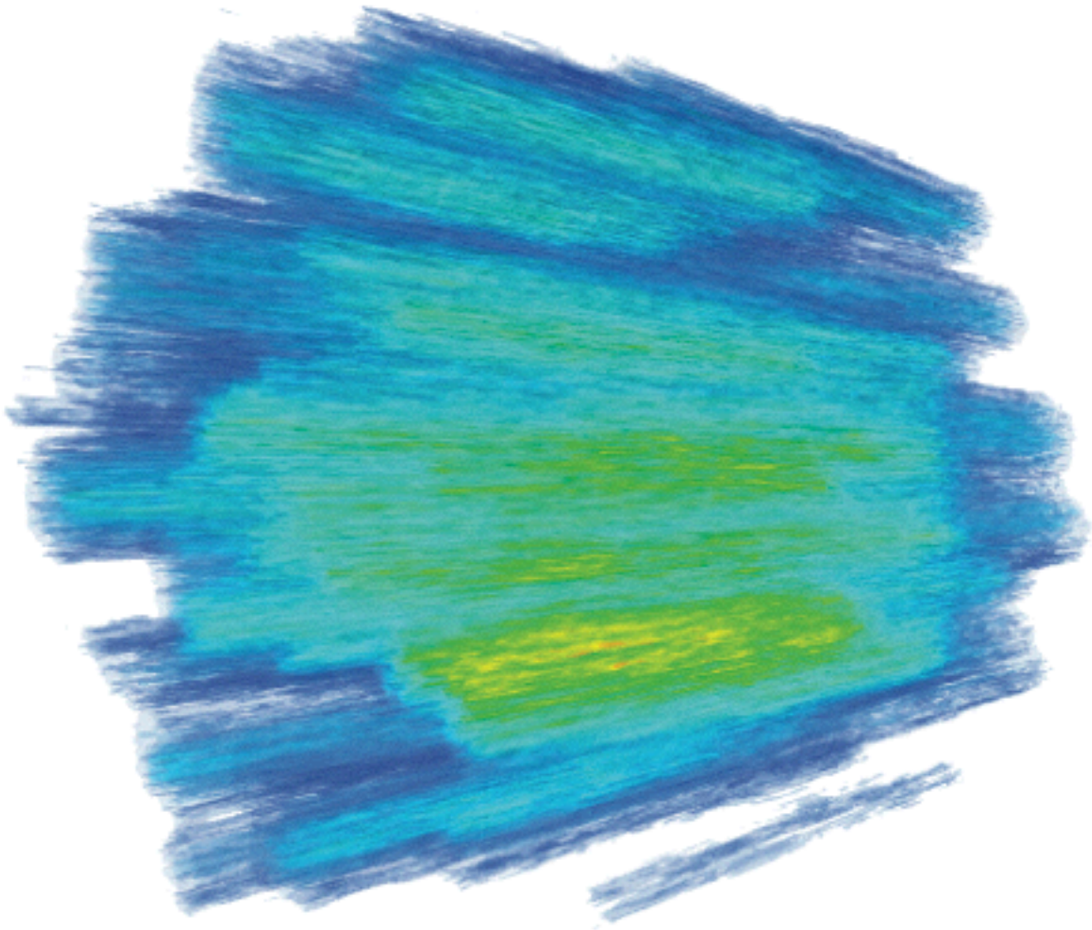

Early time dynamics and sphaleron transitions out-of-equilibrium

Early stages of HIC

colliding nuclei

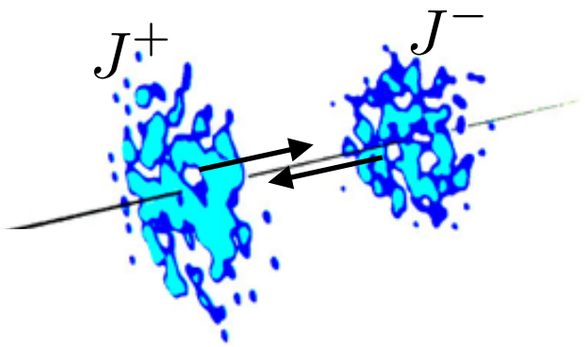

Glasma flux tubes

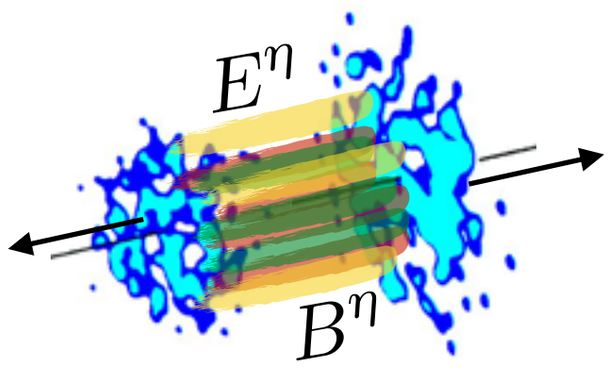

over-occupied plasma

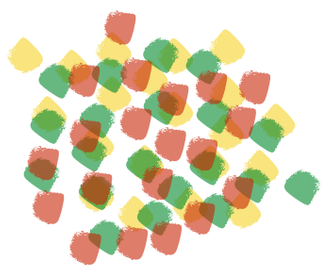

min-jets + soft bath

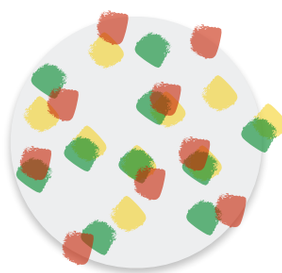

equilibrium

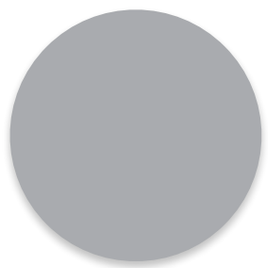

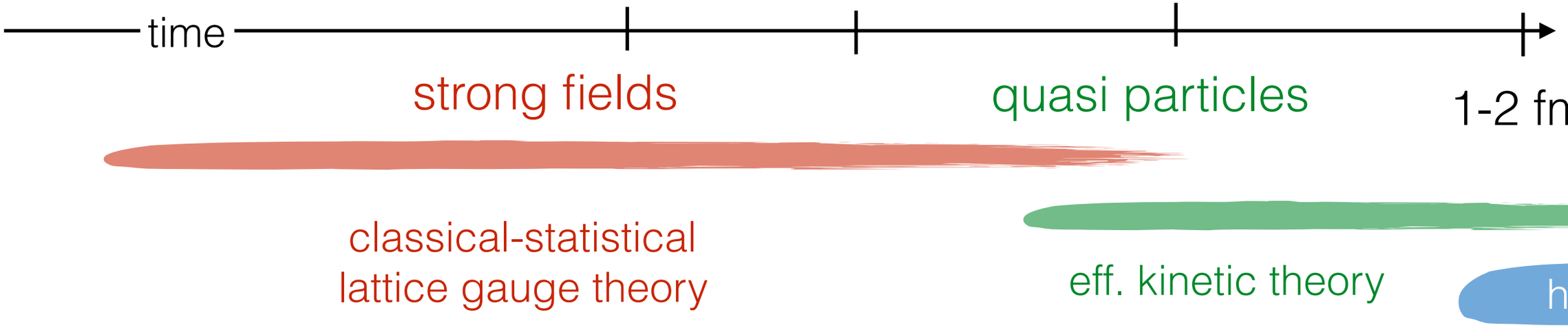

Initial state after the collision is characterized by large phase space occupancy of gluons $f(p \sim Q_s) \sim 1/\alpha_S$ with typical momentum Q_s

=> Early time dynamics described in terms of classical field dynamics

Classical Yang-Mills dynamics & topology on the lattice

Solve classical Yang-Mills equations on a space-time lattice to study non-equilibrium dynamics of Glasma (neglecting long. expansion)

Extract Chern-Simons number N_{CS} by evaluating

$$\frac{dN_{CS}}{dt} = \frac{g^2}{8\pi^2} \int d^3x \; E_i^a(\mathbf{x}) B_i^a(\mathbf{x})$$

Since local operator definition of $\vec{E}_a \cdot \vec{B}_a$ is not a total derivative on the lattice, we use cooling to remove UV fluctuations and isolate topological transitions

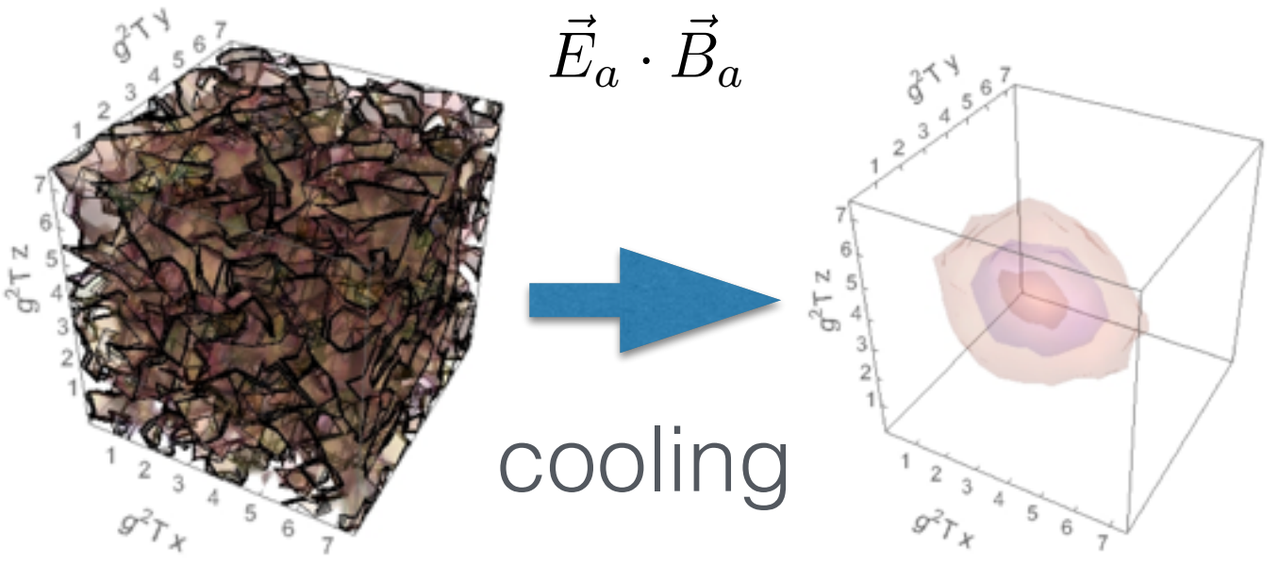

Sphaleron transitions in the Glasma

Evolution of the Chern-Simons number for a single configuration

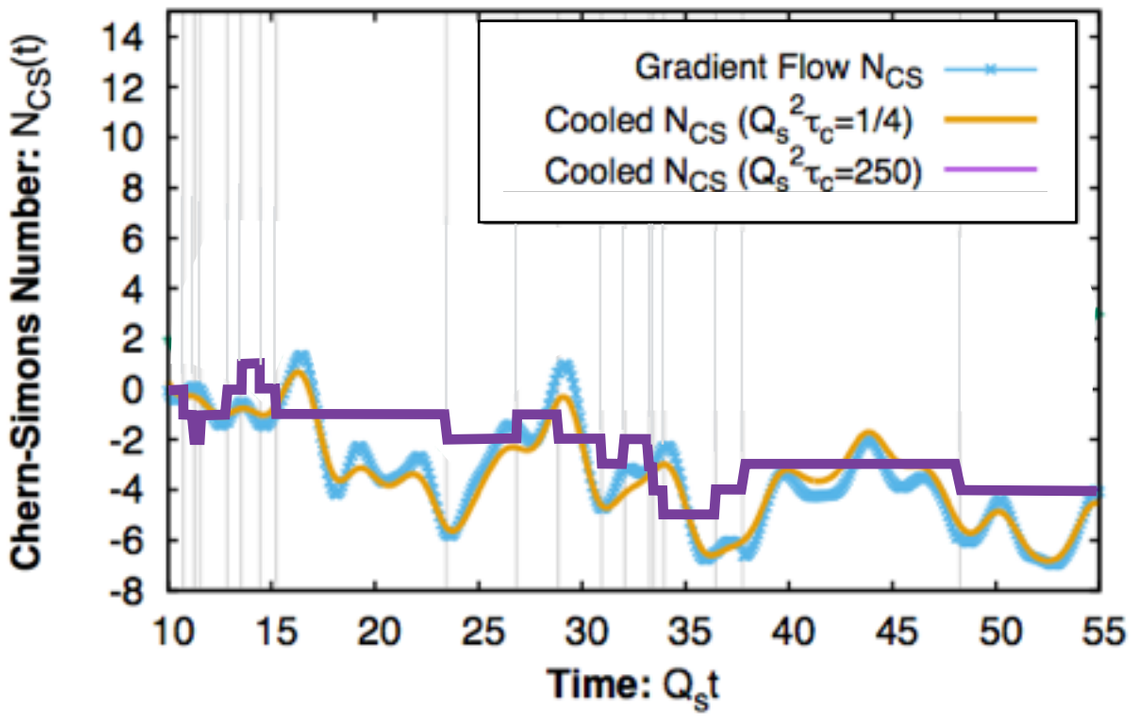

Histograms of Chern-Simons number difference

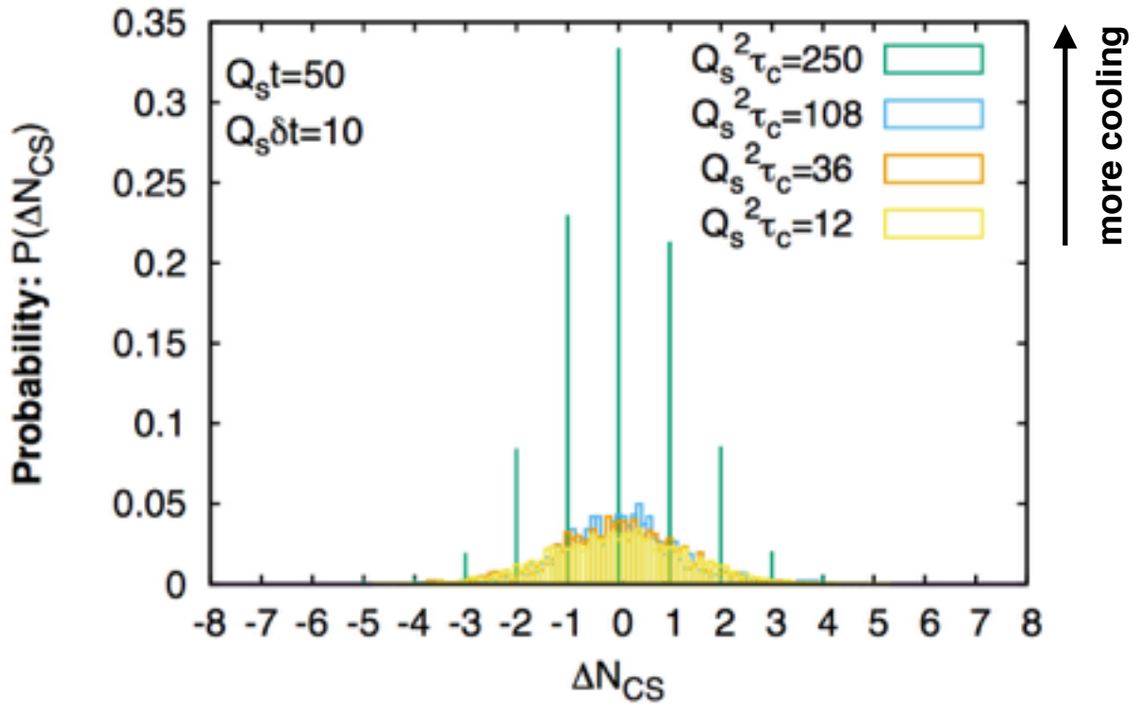

-> Can identify sphaleron transitions and separate from fluctuations by varying the amount of cooling

Mace, SS, Venugopalan PRD93 (2016) no.7, 074036

Quantifying the sphaleron rate

Extract auto-correlation function of the Chern-Simons number

$$\frac{1}{V}\left\langle \left(N_{CS}(t+\delta t) - N_{CS}(t)\right)^2 \right\rangle = \Gamma^{eq}_{sph}\delta t$$

Equilibrium:

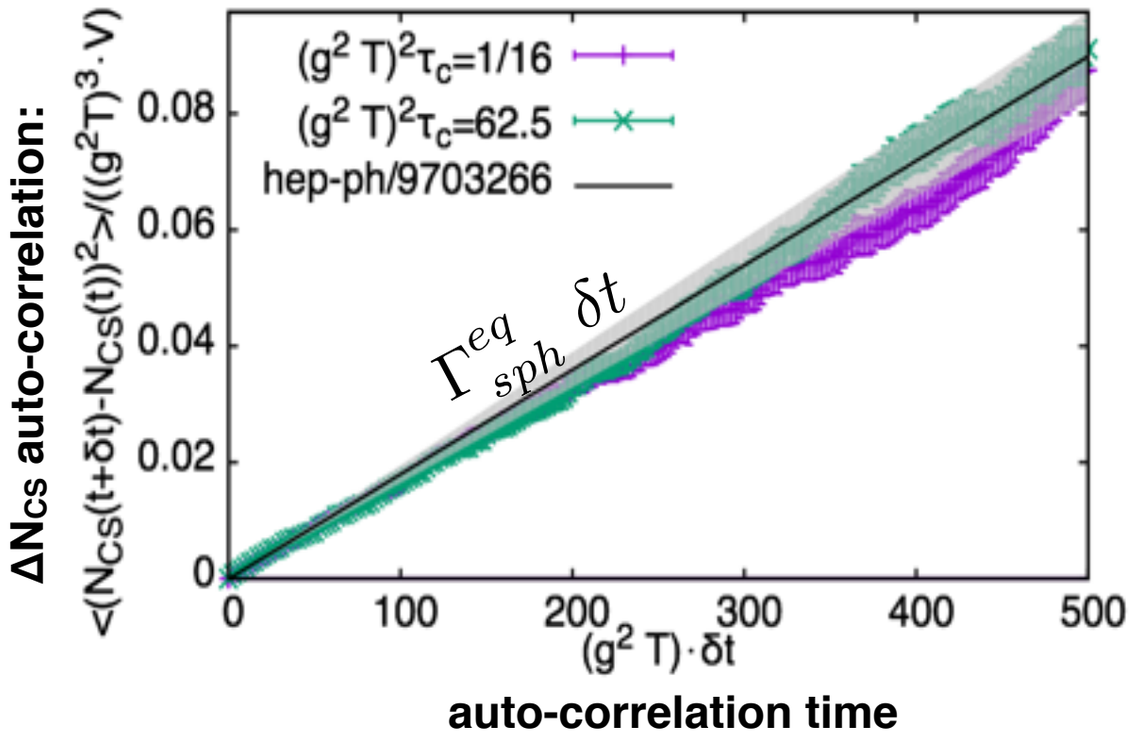

Glasma:

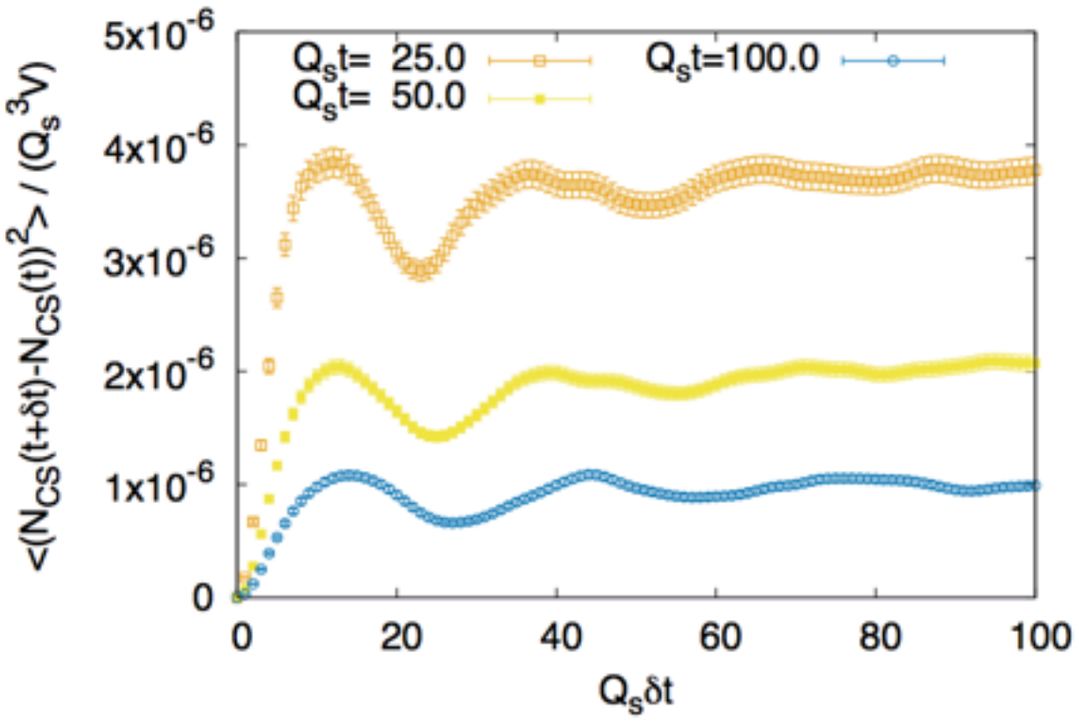

-> Simple probabilistic picture not applicable in the Glasma — clear non-Markovian emerge from the auto-correlation function

Mace, SS, Venugopalan PRD93 (2016) no.7, 074036

Quantifying the sphaleron rate

Define non-equilibrium sphaleron rate by the early rise of the auto-correlation function

$$\Gamma_{sph}^{neq}(t) = \left\langle \frac{(N_{CS}(t+\delta t) - N_{CS}(t))^2}{V\ \delta t} \right\rangle_{Q_s \delta t<10}$$

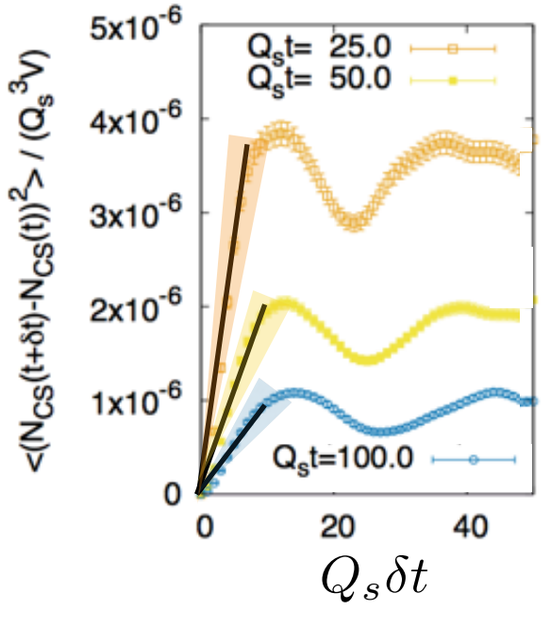

Non-equilibrium sphaleron rate

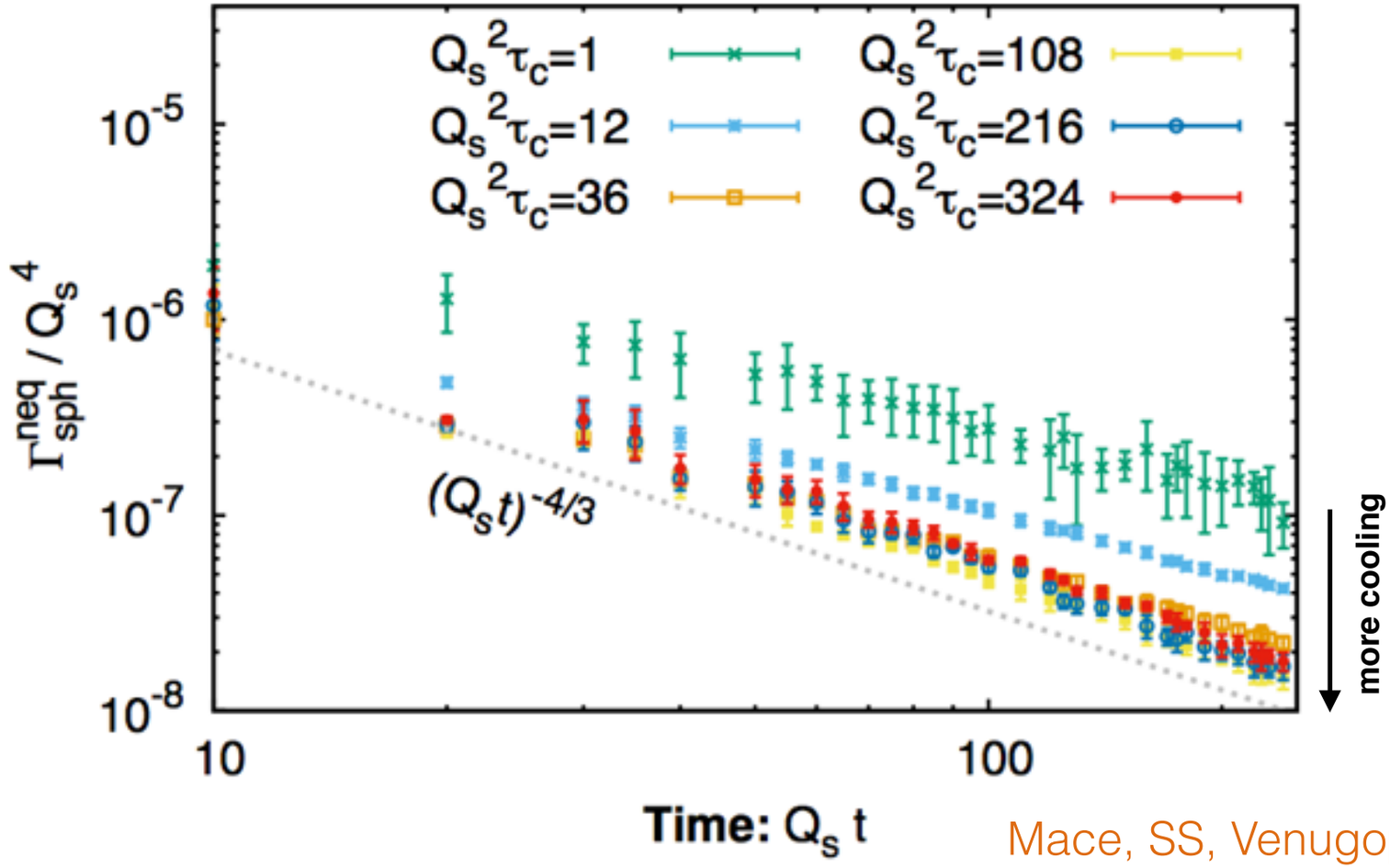

Sizable contribution from field strength fluctuations

Strong time dependence observed — rate is largest at early times and decreases rapidly as a function of time

Mace, SS, Venugopalan PRD93 (2016) no.7, 074036

Quantifying the sphaleron rate

In equilibrium sphaleron transition rate $\Gamma^{eq}_{sph} = \kappa\, \alpha_S^5 T^4$ is controlled by modes of the order of the magnetic screening length ($\sqrt{\sigma} \sim g^2T$)

Expect a more natural interpretation of Γ_{sph}/σ^2

Characteristic scales

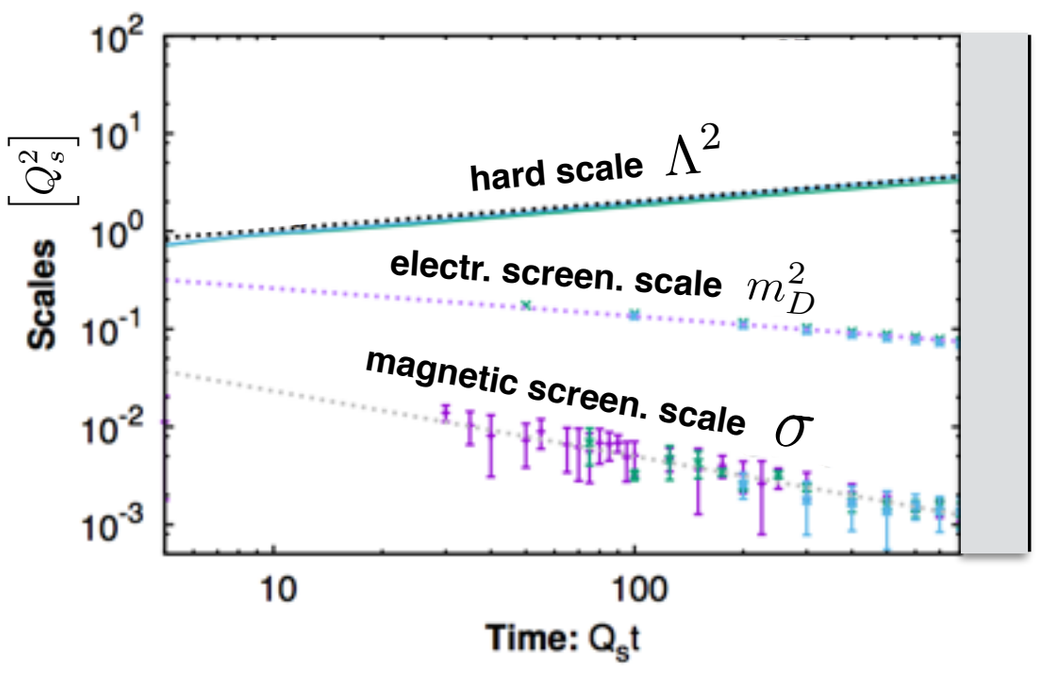

Equilibrium

$\sim T^2$

$\sim g^2T^2$

$\sim g^4T^2$

Separation of scales emerges dynamically

Sphaleron rate Γ_{sph}/σ^2

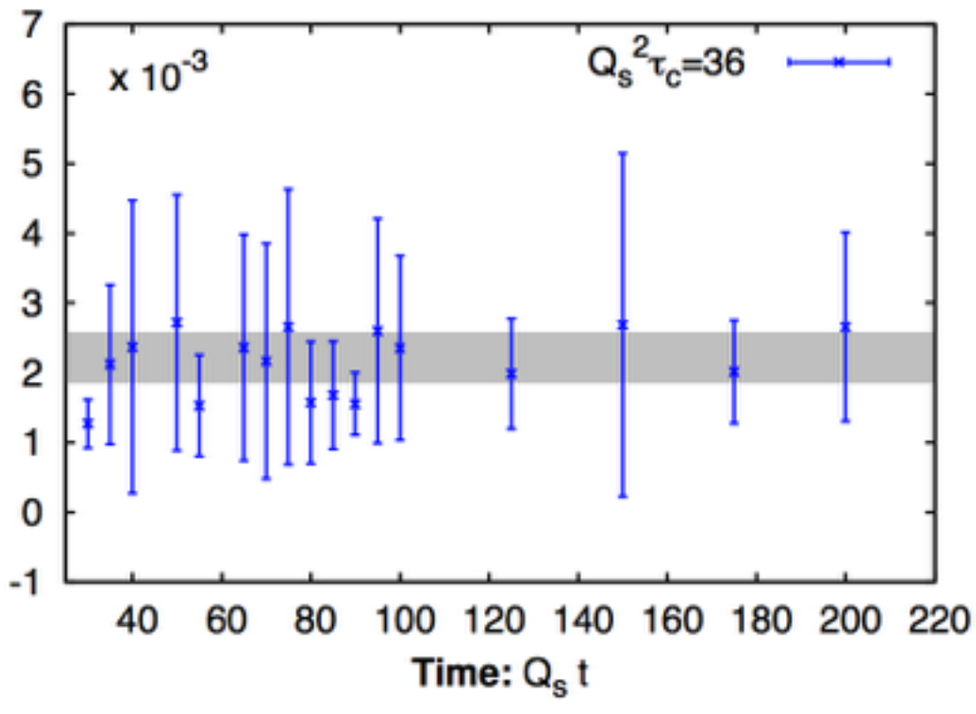

Non-equilibrium sphaleron rate dominated by modes on the order of the magnetic screening scale

Sphaleron rate in the Glasma

- Similar to the thermal case the non-equilibrium sphaleron rate is dominated by soft modes on the order of the magnetic screening scale

$$\Gamma^{neq}_{sph}(t) \approx 2 \times 10^{-3}\ \sigma^2(t) \quad \text{where} \quad \sigma^2(t) \sim Q_s^2 (Q_s t)^{-2/3}$$

for the non-expanding case.

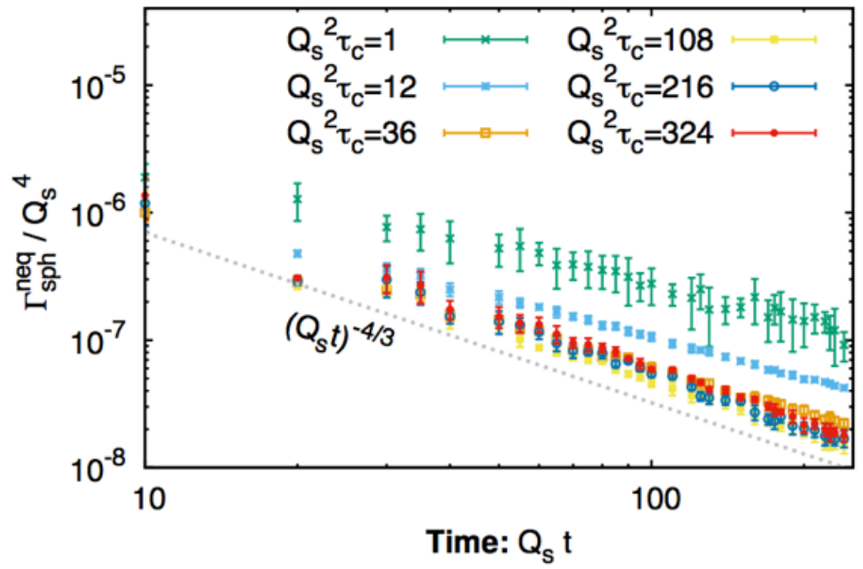

Glasma: $\Gamma^{neq}_{sph} \sim Q_s^4$ Equilibrium: $\Gamma^{eq}_{sph} \sim \alpha_S^5 T^4$

-> Early times dominate generation of axial charge imbalance

- On the time scales of interest non-equilibrium behavior of N_{CS} show qualitative differences to the thermal case

I) Significant contribution from fluctuating field strength

II) Non-Markovian nature of sphaleron transitions

- Expect qualitatively similar features when generalizing to the longitudinally expanding case relevant to HIC

3

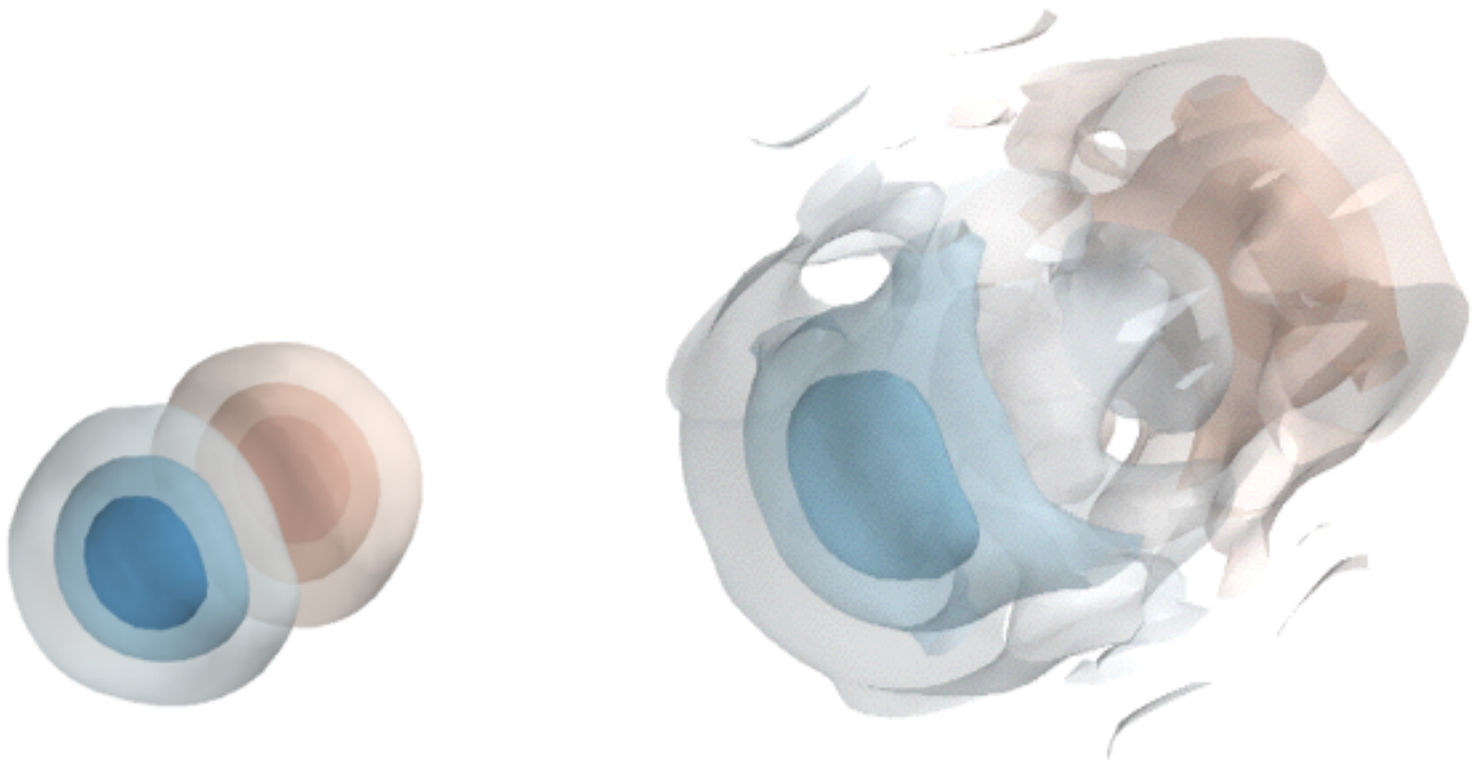

Chiral magnetic effect & anomaly induced transport from real-time lattice simulations

Non-equilibrium dynamics with fermions

Can not simply treat fermions classically, as phase-space occupancies of fermions is limited by the Pauli principle

Instead one expands the fermion field in operator basis at initial time

$$\hat{\psi}(x,t) = \sum_{p,\lambda} \hat{b}_{p,\lambda}(t=0)\phi_u^{p,\lambda}(x,t) + \hat{d}^{\dagger}_{p,\lambda}(t=0)\phi_v^{p,\lambda}(x,t)$$

and evolves the wave-functions by solving the Dirac equation

$$(i\not{D}_w - m)\hat{\psi} = 0 \qquad \not{D}_w \quad \text{coupling to QCD +QED fields}$$

measure operator expectation values

$$j_V^{\mu} = e\ \langle \hat{\bar{\psi}}(x)\gamma^{\mu}\hat{\psi}(x)\rangle$$

Straightforward to include back reaction to gauge sector $D_\mu F^{\mu\nu} = j^{\nu}$

So far only studied quenched dynamics in the presence of sphaleron transition and an external magnetic field

Axial anomaly in real-time

Non-trivial realization of axial anomaly for Wilson fermions which requires decoupling of fermion doublers

Karsten, Smit Nucl. Phys. B183 (1981) 103

$$\partial_\mu j_5^\mu(x) = 2m < \bar{\psi}(x) i\gamma_5 \psi(x) > + r_W < W(x) > \rightarrow -\frac{g^2}{8\pi^2} \mathrm{Tr} F_{\mu\nu} F^{\mu\nu}$$

Cross-check anomaly with improved Wilson and overlap fermions

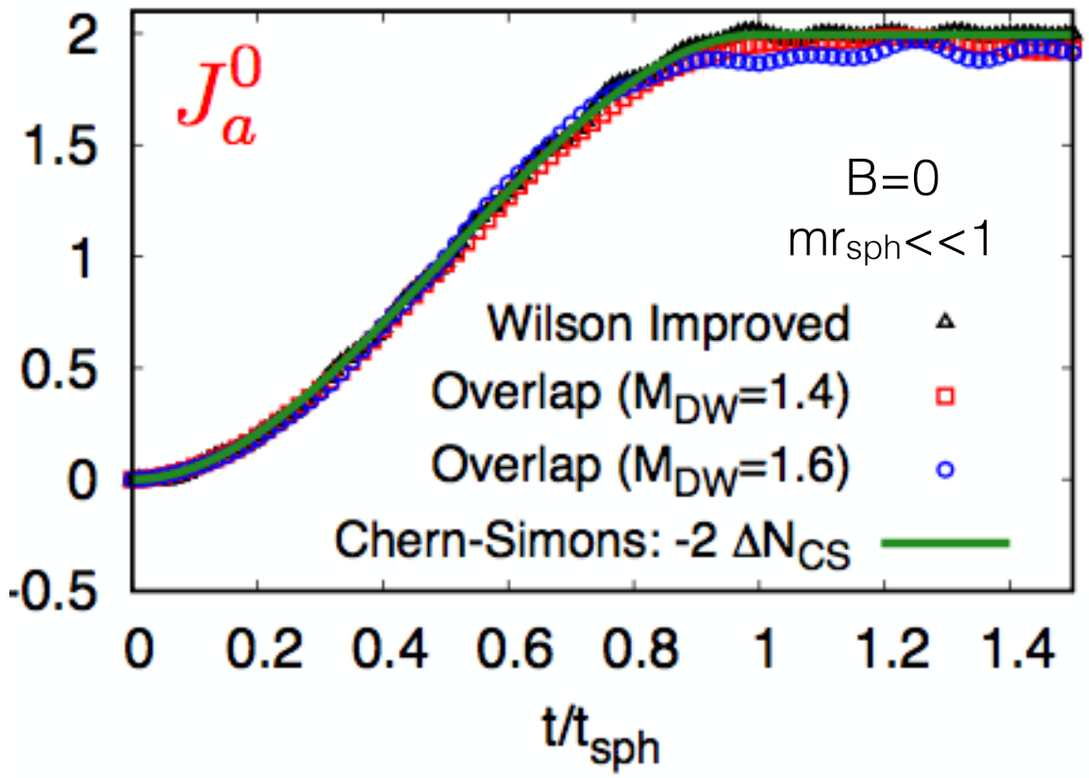

Sphaleron transition leads to a unit change of Chern-Simons number

$$\Delta N_{CS} = \frac{g^2}{8\pi^2} \int d^4x \; \vec{E}_a \vec{B}_a$$

an induces an imbalance of axial charge

$$\Delta J_5^0 = -2\Delta N_{CS} + 2m_f \int d^4x \langle \bar{\psi} i\gamma_5 \psi \rangle$$

(M.Mace,N.Mueller,SS, S. Sharma in preparation)

CME Dynamics

Sphaleron transition induces local imbalance
of axial charge density j_5^0

Axial charge j_5^0 Vector current j_V^z Vector charge j_V^0

Non-zero magnetic field B_z -> vector current j_V^z is generated

Vector current j_V^z leads to separation of electric charges j_V^0
along the B-field direction

(N.Mueller,SS, S. Sharma arXiv:1606.00342)

CME Dynamics

Sphaleron transition induces local imbalance
of axial charge density j_5^0

Axial charge j_5^0 Vector current j_V^z Vector charge j_V^0

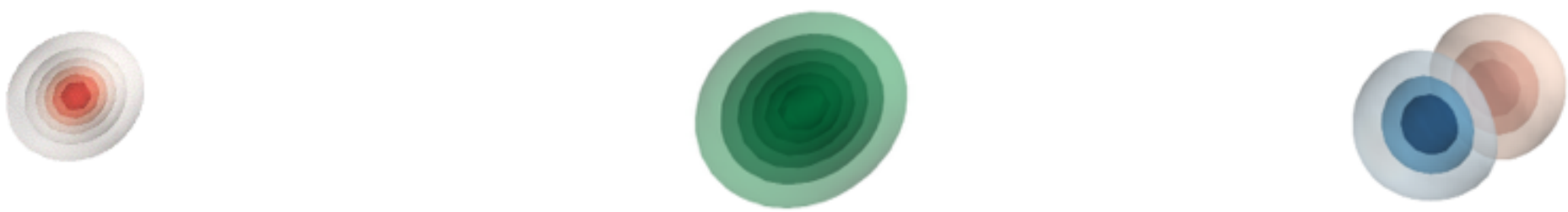

Non-zero magnetic field B_z -> vector current j_V^z is generated

Vector current j_V^z leads to separation of electric charges j_V^0
along the B-field direction

(N.Mueller,SS, S. Sharma arXiv:1606.00342)

CME Dynamics

Sphaleron transition induces local imbalance
of axial charge density j_5^0

Axial charge j_5^0 Vector current j_V^z Vector charge j_V^0

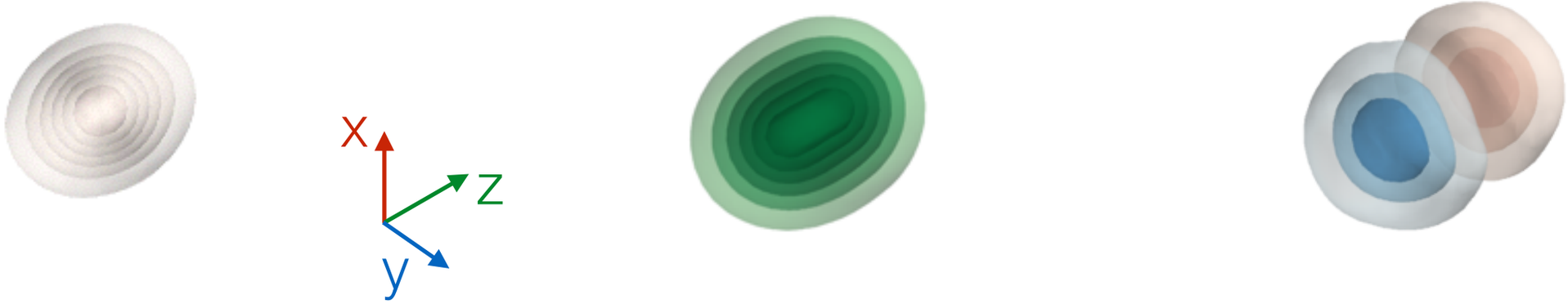

Non-zero magnetic field B_z -> vector current j_V^z is generated

Vector current j_V^z leads to separation of electric charges j_V^0
along the B-field direction

(N.Mueller,SS, S. Sharma arXiv:1606.00342)

CMW Dynamics

Vector charge imbalance j_V^0 generates an axial current j_5^z
so that axial charge also flows along the B-field direction

Axial charge j_5^0 Vector current j_V^z Vector charge j_V^0

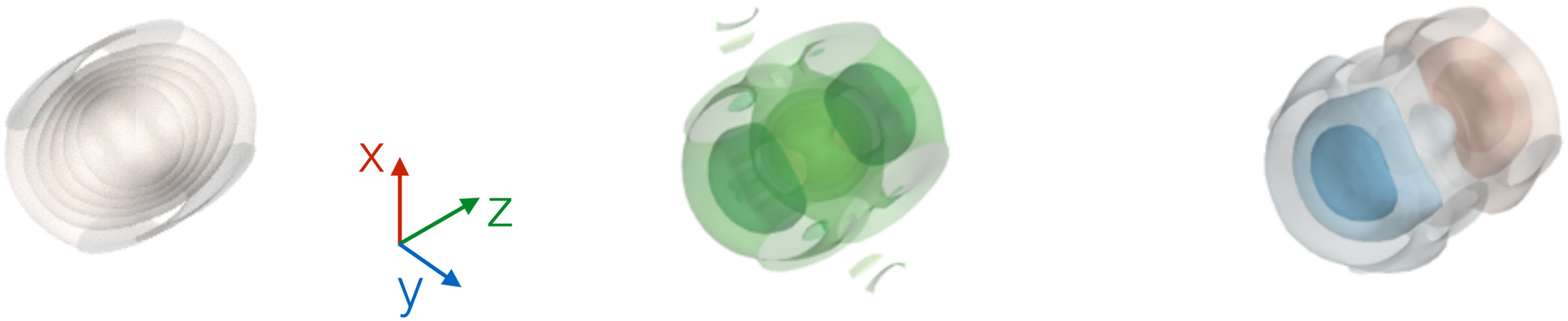

Shock-wave of vector charge and axial charge
propagating along B-field direction

(N.Mueller,SS, S. Sharma arXiv:1606.00342)

CMW Dynamics

Vector charge imbalance j^0_V generates an axial current j^z_5
so that axial charge also flows along the B-field direction

Axial charge j^0_5 Vector current j^z_V Vector charge j^0_V

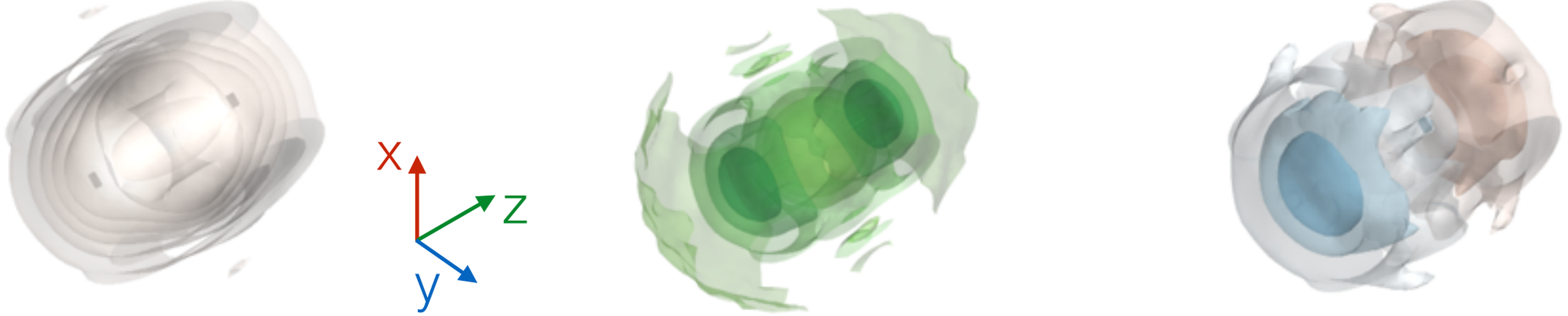

Shock-wave of vector charge and axial charge
propagating along B-field direction

(N.Mueller,SS, S. Sharma arXiv:1606.00342)

CMW Dynamics

Vector charge imbalance j_V^0 generates an axial current j_5^z
so that axial charge also flows along the B-field direction

Axial charge j_5^0 Vector current j_V^z Vector charge j_V^0

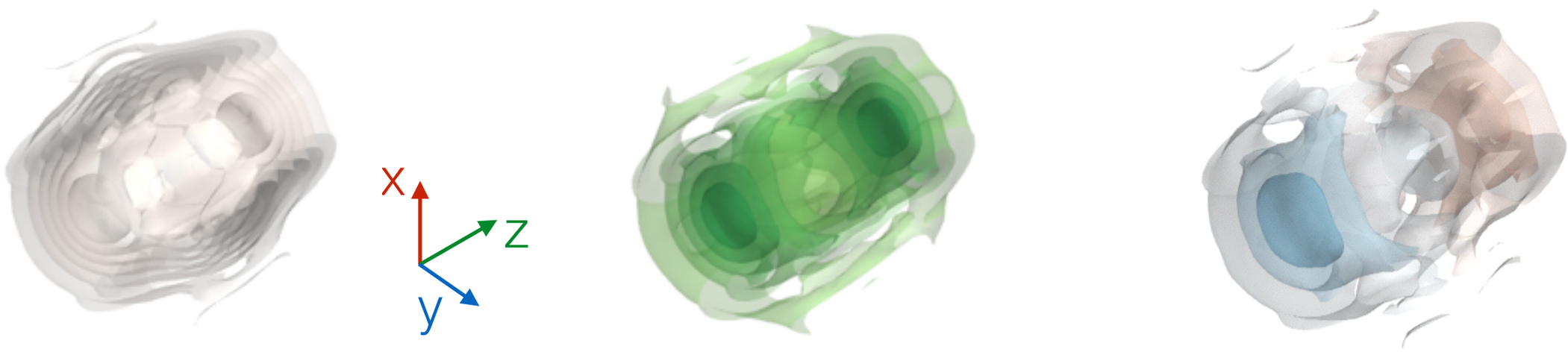

Shock-wave of vector charge and axial charge
propagating along B-field direction

(N.Mueller,SS, S. Sharma in preparation)

Non-equilibrium CME dynamics

Axial charge j_5^0

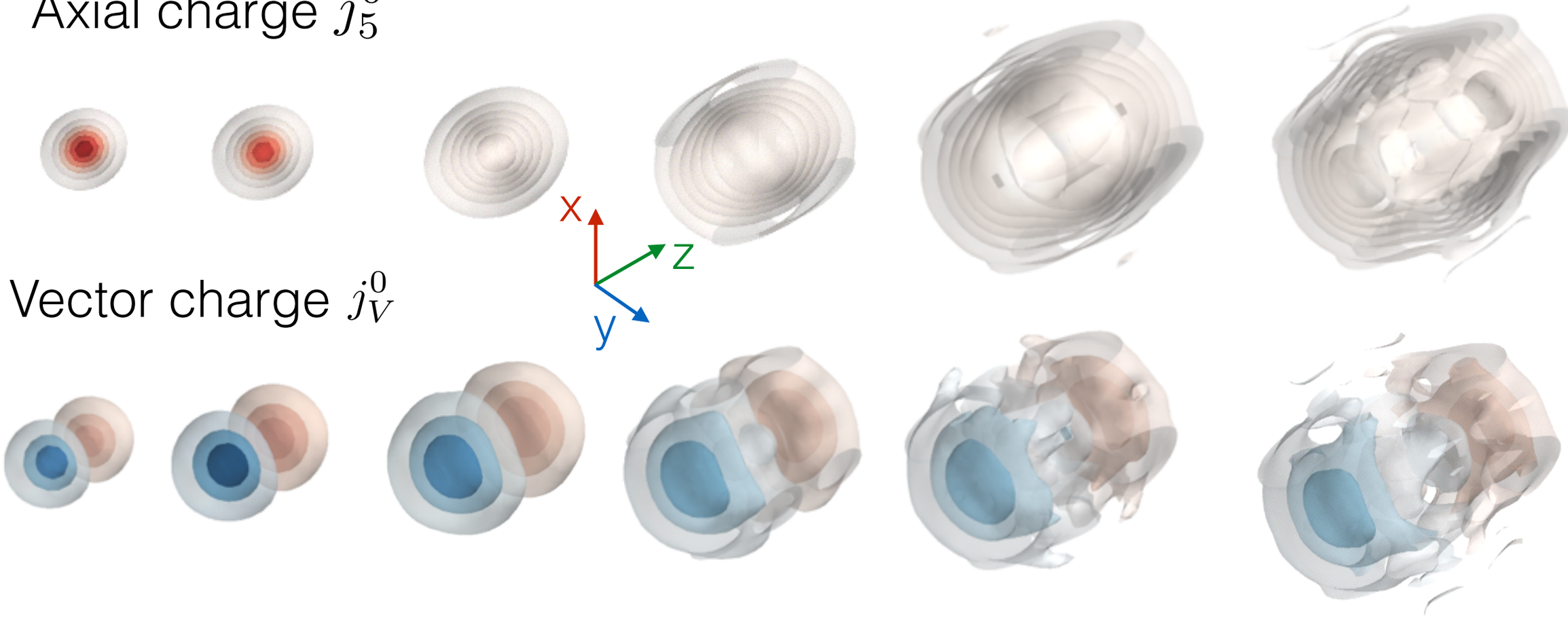

Vector charge j_V^0

Clear separation of electric charge j_V^0 along the B-field direction

First time anomalous transport phenomena have been confirmed from non-perturbative real-time lattice simulations

(N.Mueller, SS, S. Sharma arXiv:1606.00342)

Non-equilibrium CME dynamics

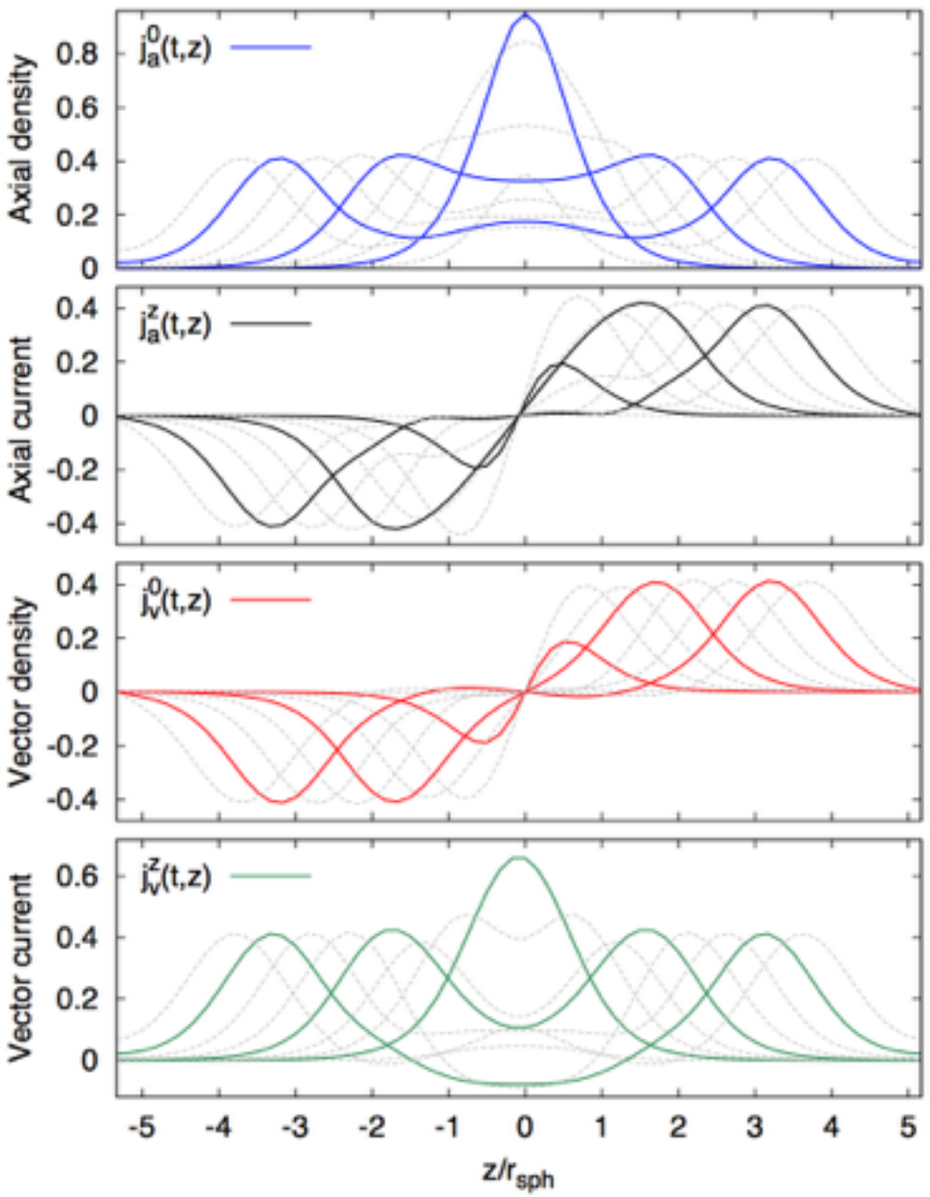

Comparison with
anomalous hydrodynamics

$$j^{\mu}_{v,a} = n_{v,a}u^{\mu} + D_{v,a}\nabla^{\mu}n_{v,a} + \sigma^{B}_{v,a}B^{\mu}$$

Strong field limit ($B \gg r_{\rm sph}^{-2}, m^2$)

$$\partial_t \begin{pmatrix} j^0_v(t,z) \\ j^0_a(t,z) \end{pmatrix} = -\partial_z \begin{pmatrix} j^0_a(t,z) \\ j^0_v(t,z) \end{pmatrix} + \begin{pmatrix} 0 \\ S(t,z) \end{pmatrix}$$

Shock-wave solutions

$$j^0_{v,a}(t > t_{\rm sph}, z) = \qquad (9)$$
$$\frac{1}{2}\int_0^{t_{\rm sph}} dt' \left[S\big(t', z - c(t-t')\big) \mp S\big(t', z + c(t-t')\big)\right]$$

(N.Mueller, SS, S. Sharma arXiv:1606.00342)

Quark mass dependence

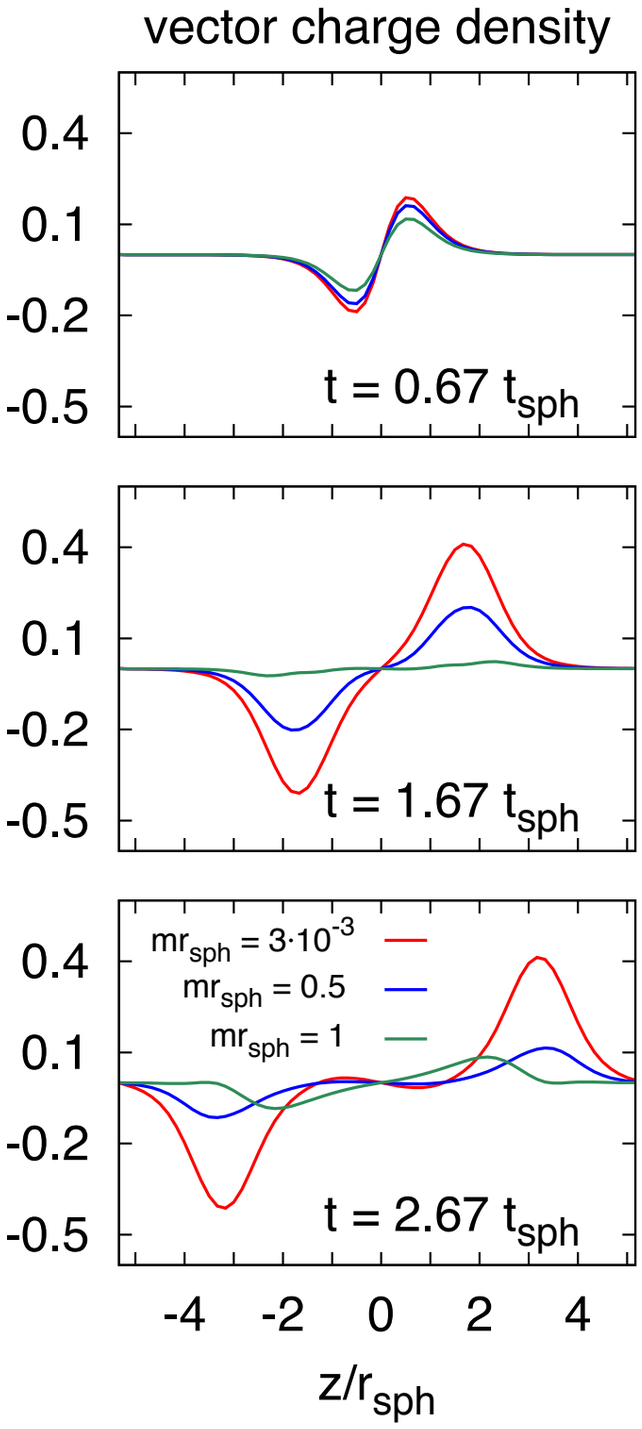

Light quarks (mr_{sph}<<1)

Chiral magnetic wave leads to non-dissipative transport of axial and vector charges

Evolution at late times well described by anomalous hydrodynamics

Heavy quarks (mr_{sph}~1)

Dissipation of axial charge leads to significant reduction of axial charge density already for mr_{sph}~1

How to include dissipative effects into macroscopic description?

(M.Mace, N.Mueller, SS, S. Sharma in preparation)

Spectral properties

Goal: Explore spectral properties to verify intuitive pictures

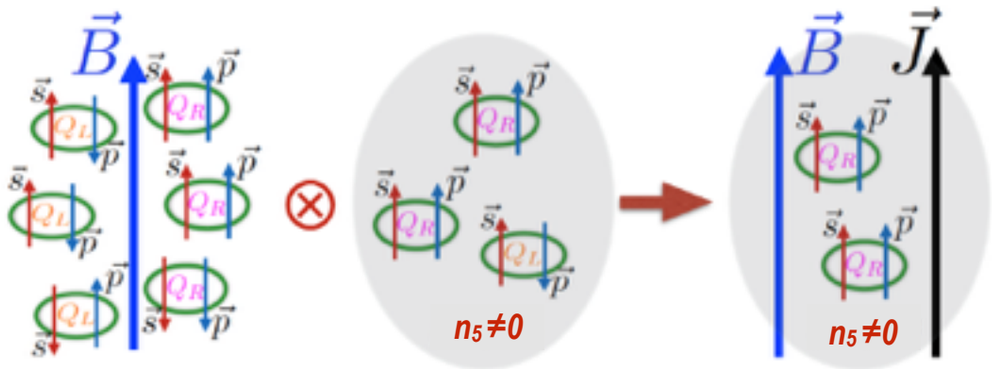

Kharzeev, Liao, Voloshin, Wang
Prog. Part. Nucl. Phys. 88 (2016) 1-28

Defined from projection of gauge invariant two-point correlation function onto quasi-particle states

$$n_h^u(p) = \int u_p^{(h)} \langle \psi^\dagger(x) U_{xy} \psi(y) \rangle u_p^{\dagger(h)} \; e^{-ip(x-y)}$$

So far only implemented for B=0 (work in progress)

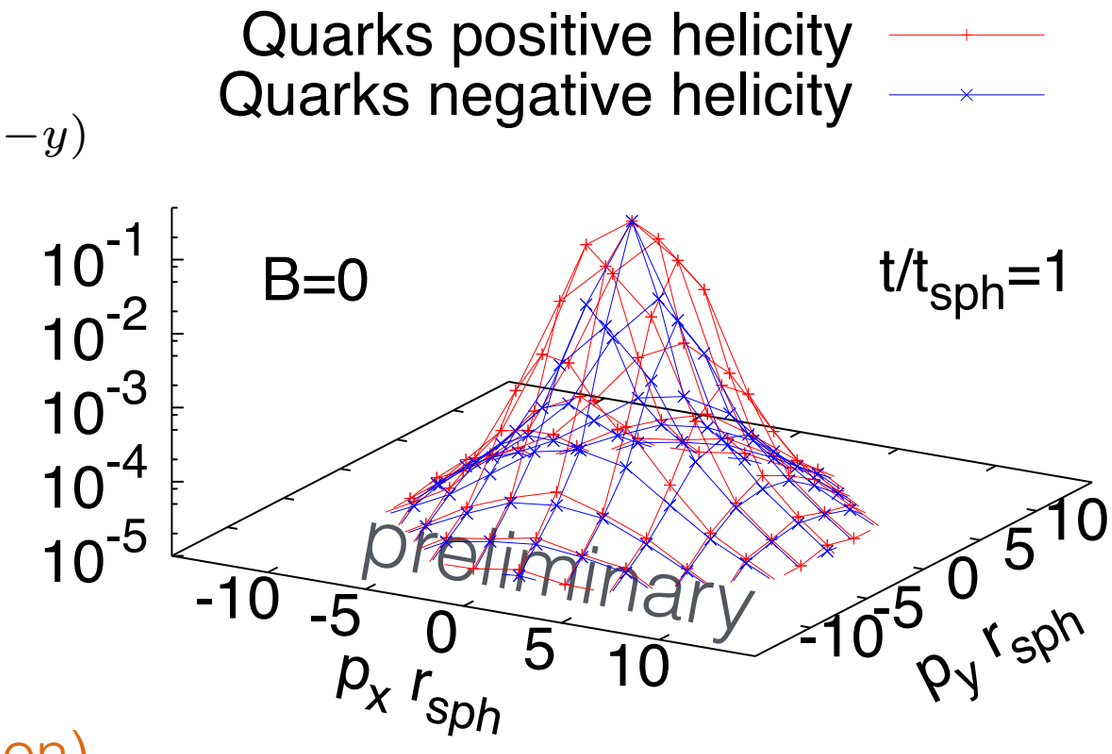

(M.Mace, N.Mueller, SS, S. Sharma in preparation)

Conclusions & Outlook

Sphaleron transition rate enhanced during the early stages of HIC

Developed of real-time lattice techniques to study dynamics of vector and axial charges out-of-equilibrium

First confirmation of CMW from real-time lattice simulations

Extend simulations to include back-reaction and study quark production for realistic gauge field configurations

Ultimate goal to provide initial conditions for anomalous hydrodynamics is within reach

Expect several applications beyond high-energy QCD

Dirac semi-metals

Backup

Early times ($0 < Q_s\tau < 1$)

Strong boost invariant classical fields E^η, B^η created immediately after the collision

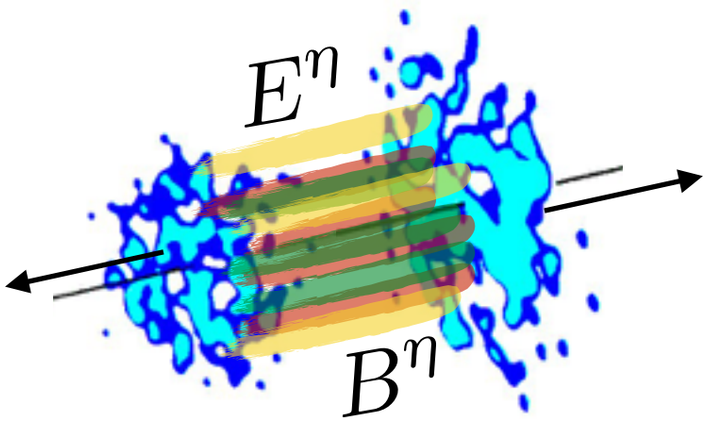

Decoherence of classical fields occurs on a time scale $1/Q_s$

- next-to-leading order (α_s) corrections break boost invariance

  -> plasma instabilities lead to an increase of longitudinal pressure

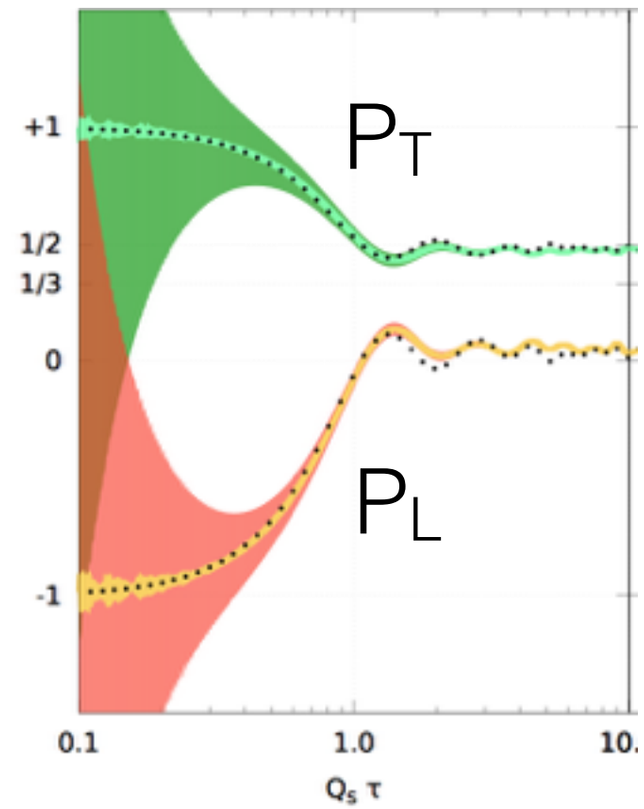

(Epelbaum,Gelis PRL 111 (2013) 232301,
Berges, Schenke, SS , Venugopalan NPA 931 (2014) 348-353)

Classical regime ($1<Q_s\tau<\alpha_s^{-3/2}$)

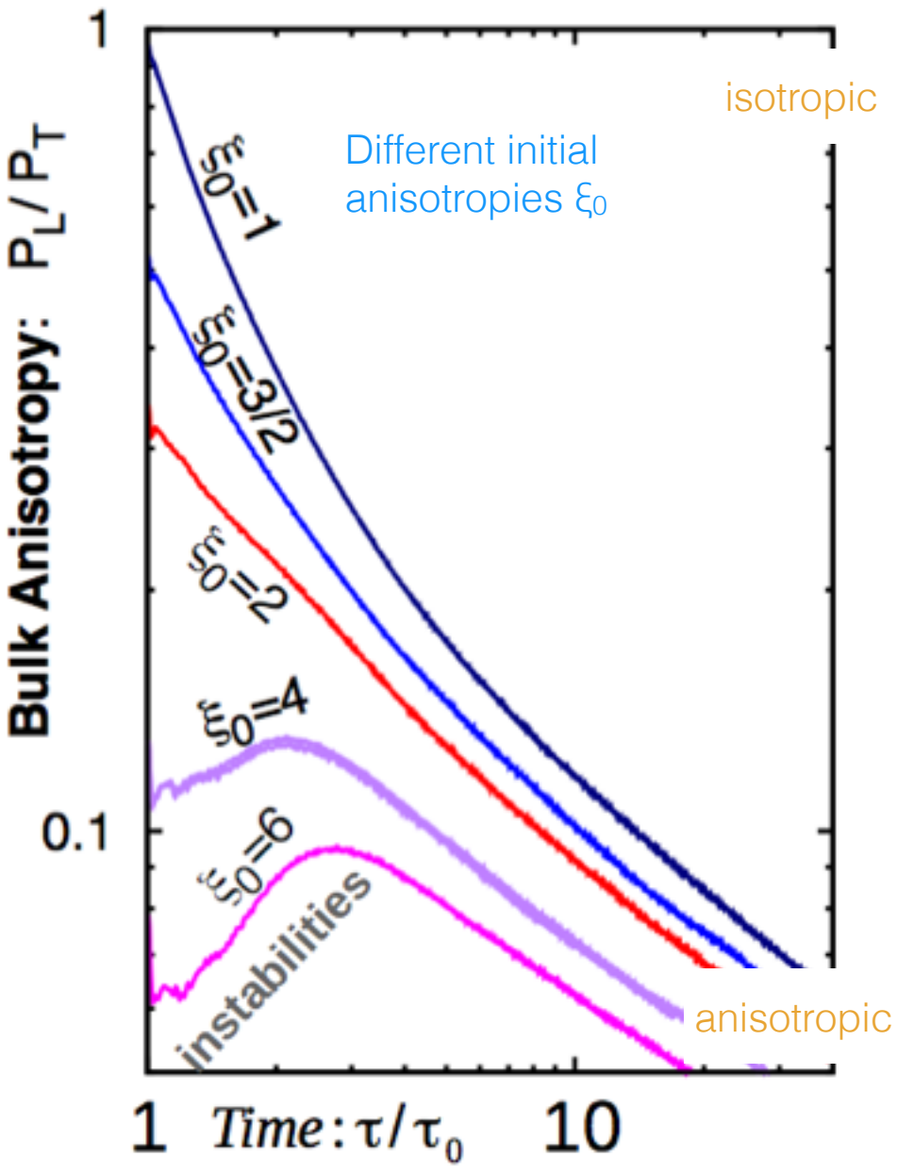

Classical field interactions are not sufficiently strong to restore isotropy beyond $1/Q_s$

-> anisotropy of the plasma increases again

No sign of plasma instabilities playing a significant role at later times $Q_s\tau > 1$

(Berges, Boguslavski, SS, Venugopalan PRD 89 (2014) 074011; 89 (2014) 114007)

Classical regime ($1<Q_s\tau<\alpha_s^{-3/2}$)

Classical field evolution ($\tau>1/Q_s$) of hard modes can be accurately described in terms of weakly interacting quasi particles

-> classical particle/field duality

Effective kinetic description
(Arnold, Morre, Yaffe JHEP 0301 (2003) 030)

$$\frac{df}{dt} = -C_{2\leftrightarrow 2}[f] - C_{1\leftrightarrow 2}[f]$$

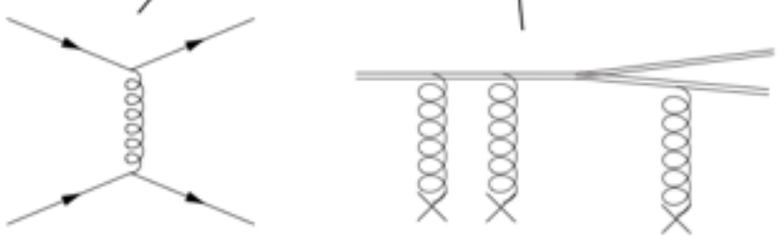

Kinetic theory

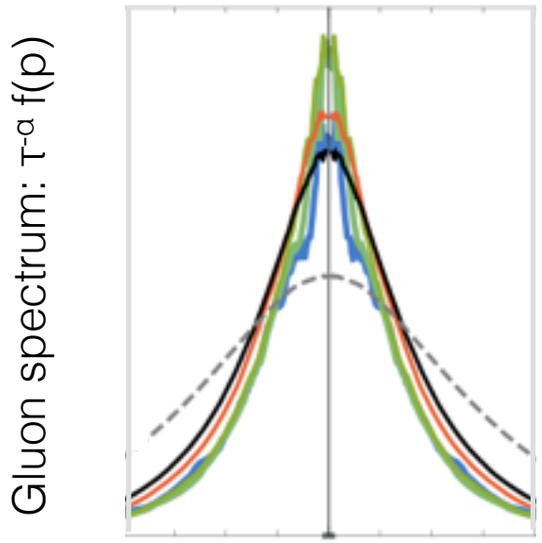

Kurkela, Zhu
PRL 115 (2015) 182301

Classical Yang-Mills

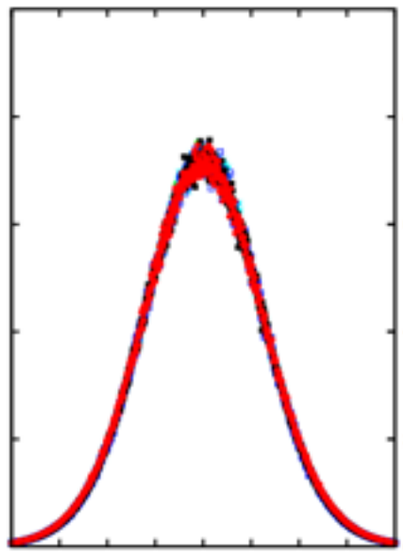

Berges, Boguslavski, SS, Venugopalan
PRD 89 (2014) 074011

-> Effective kinetic description (AMY) can be used to study dynamics of hard modes from $\tau > 1/Q_s$ all the way to equilibration

Bottom-up scenario

Equilibration process beyond $\tau \sim 1/Q_s$ occurs as a three step process
(Baier et al. PLB 502 (2001) 51-58)

Kurkela arXiv:1601.03283

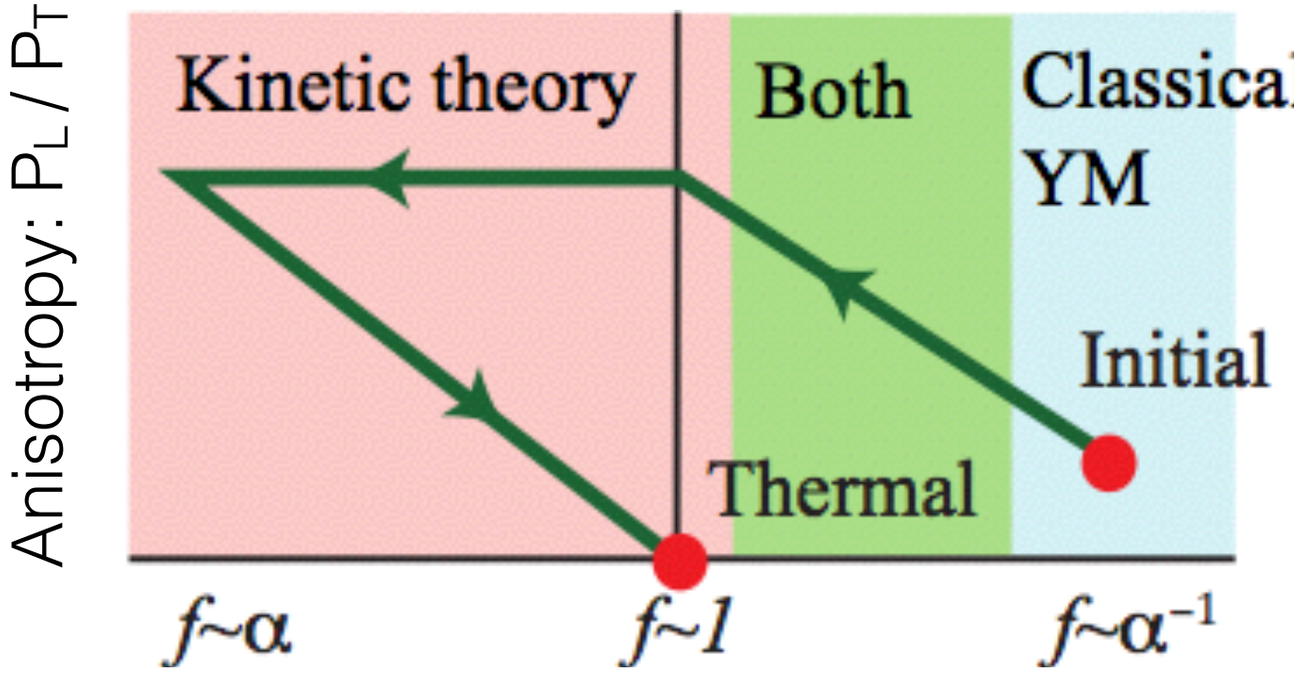

Berges, Boguslavski, SS, Venugopalan
PRD 89 (2014) 074011

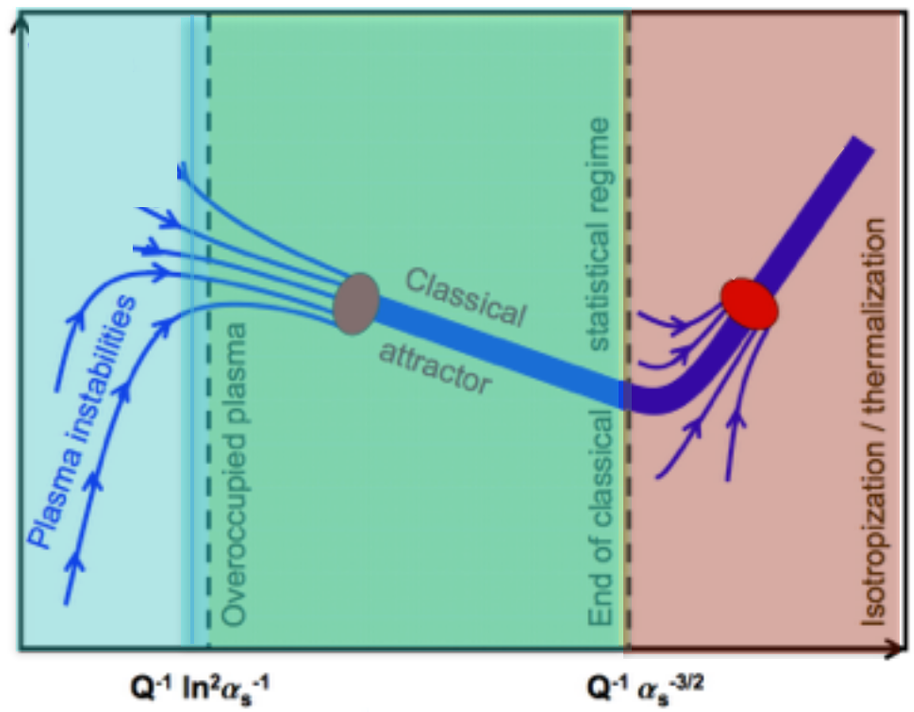

Need to switch from classical Yang-Mills to kinetic description
to describe approach to equilibrium

Quantum regime ($Q_s\tau>\alpha_s^{-3/2}$)

Inelastic processes dominate and lead to a radiative break-up

-> mini-jets loose all their energy to soft thermal bath

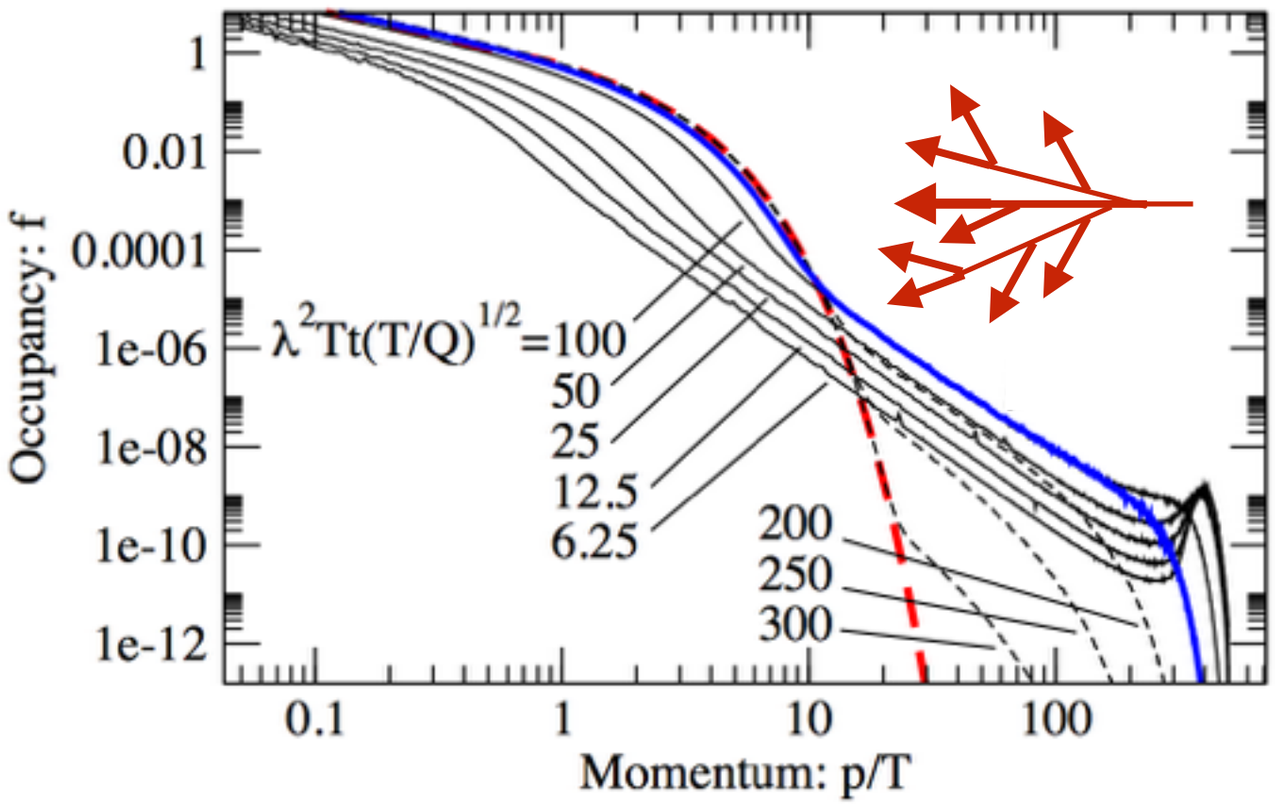

Kurkela, Lu PRL 113 (2014) 182301

equilibration <-> (mini-) jet quenching

Quantum regime ($Q_s\tau>\alpha_s^{-3/2}$)

Inelastic processes dominate and lead to a radiative break-up

-> mini-jets loose all their energy to soft thermal bath

Soft bath heating up due to energy deposited by mini-jets

-> longitudinal pressure rises and system isotropizes

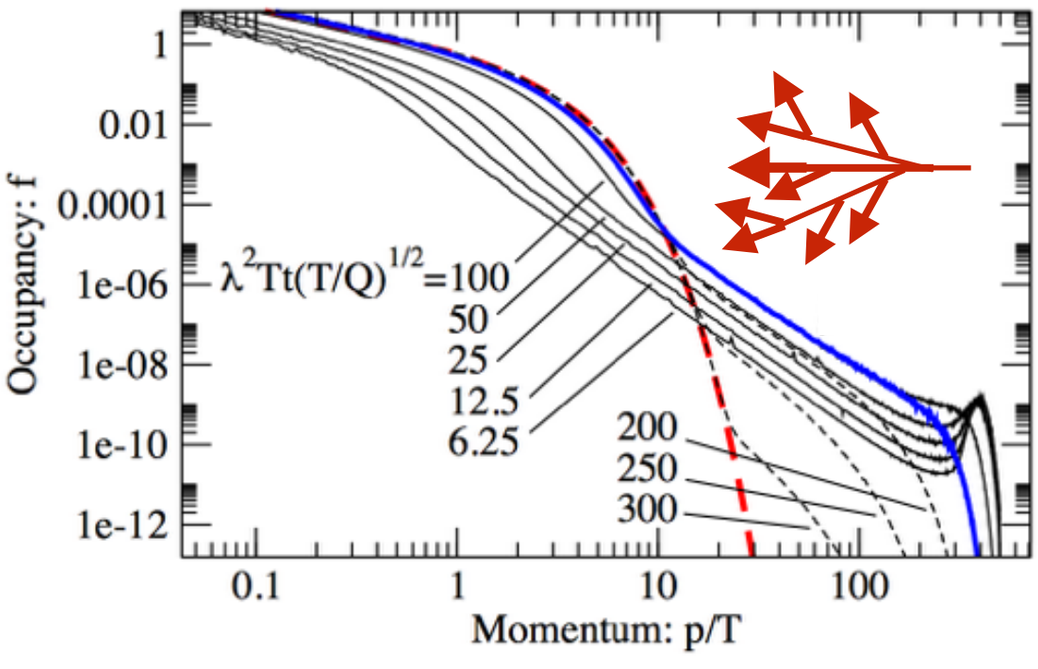

Kurkela, Lu PRL 113 (2014) 182301

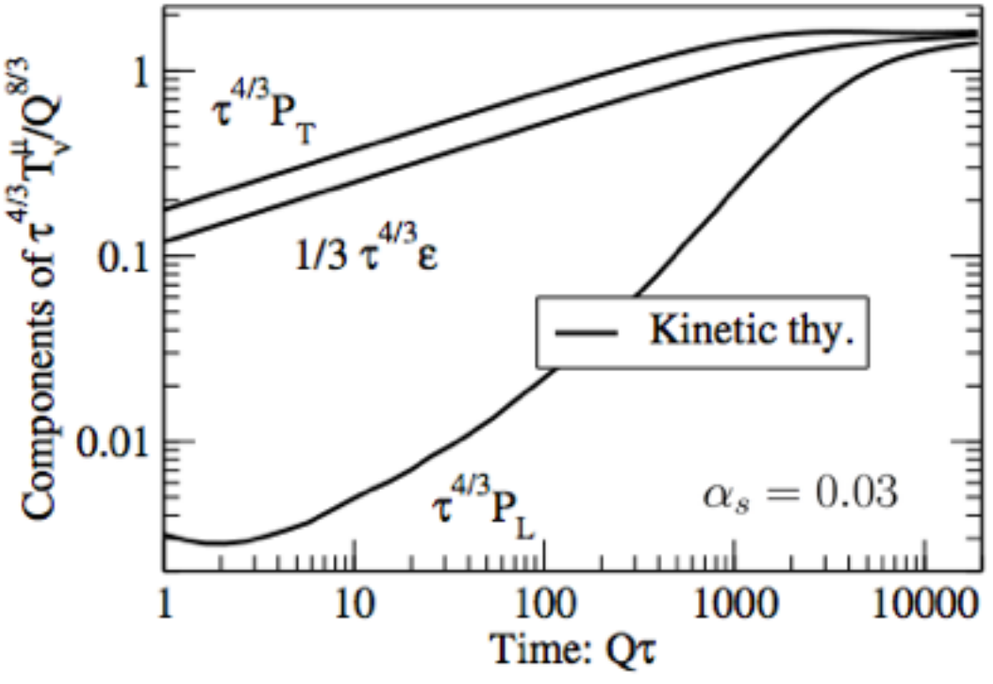

Kurkela, Zhu PRL 115 (2015) 182301

Quantum regime ($Q_s\tau > \alpha_s^{-3/2}$)

Inelastic processes dominate and lead to a radiative break-up

-> mini-jets loose all their energy to soft thermal bath

Soft bath heating up due to energy deposited by mini-jets

-> longitudinal pressure rises and system isotropizes

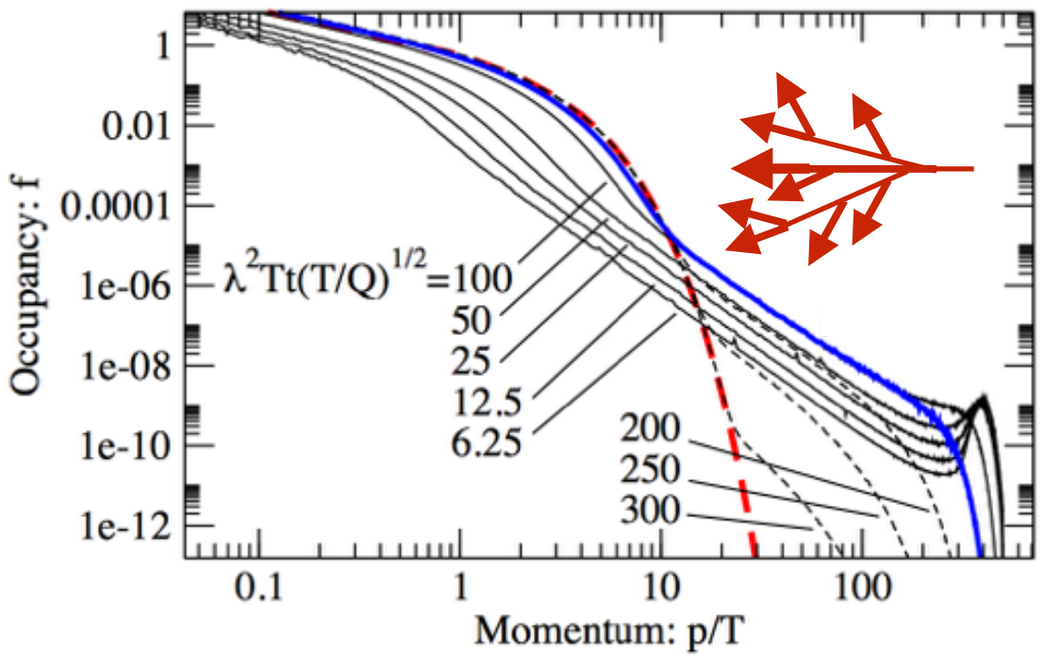

Kurkela, Lu PRL 113 (2014) 182301

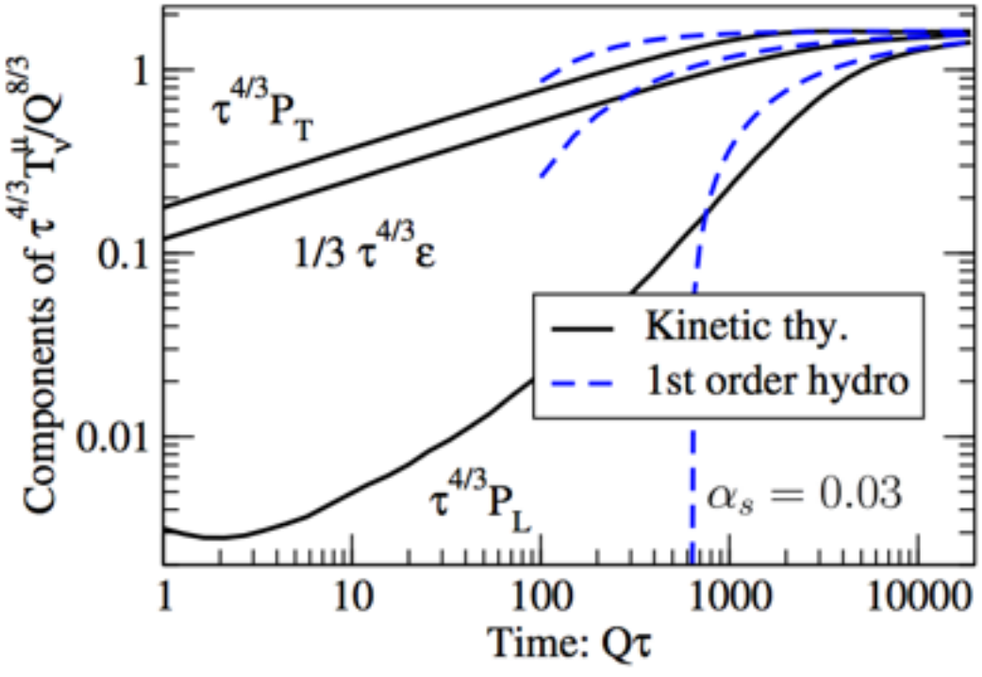

Kurkela, Zhu PRL 115 (2015) 182301

-> smooth matching to hydro-dynamics (no free parameters)

Equilibration process

Clear understanding of the dynamics in the weak-coupling limit

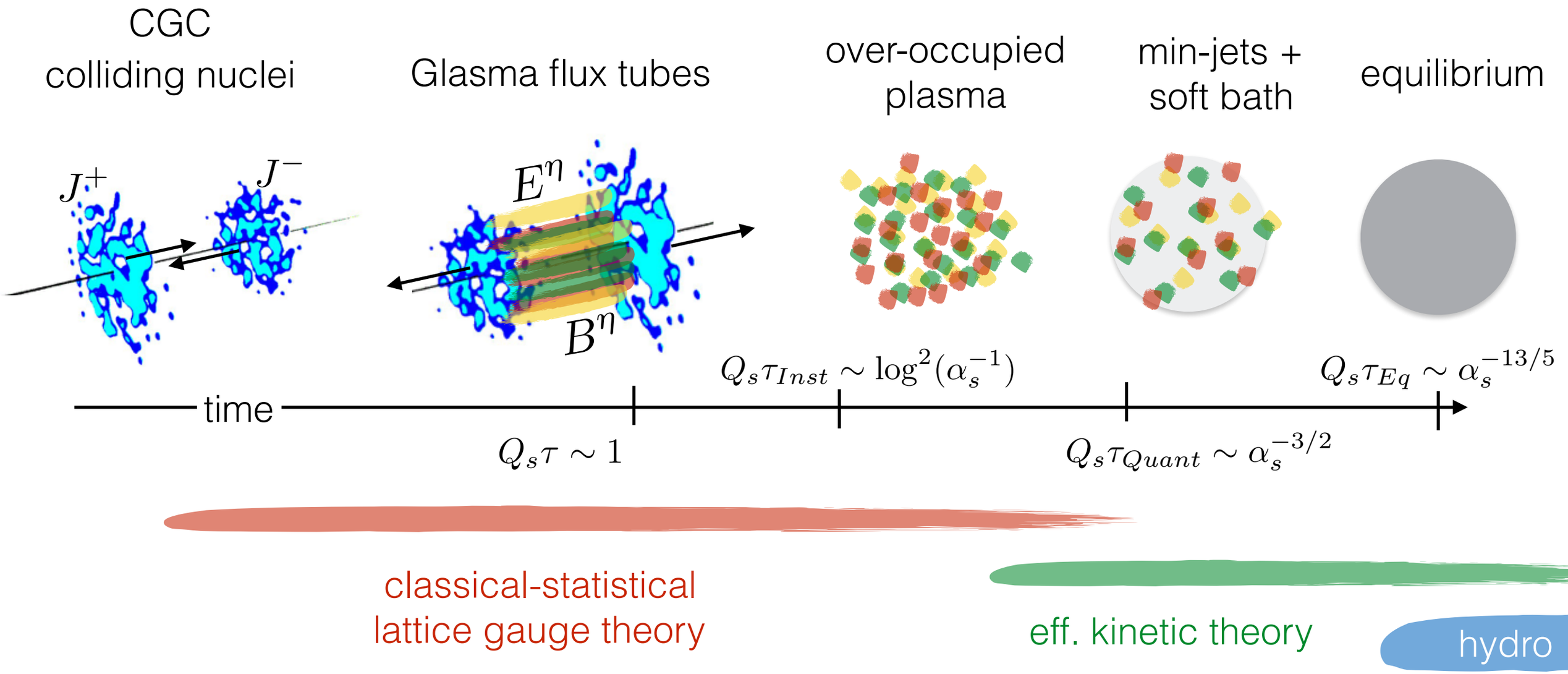

Developed the tools to compute equilibration process from combination of weak-coupling methods

Beyond weak coupling

Extrapolate leading order weak coupling description to physical values α_s=0.3

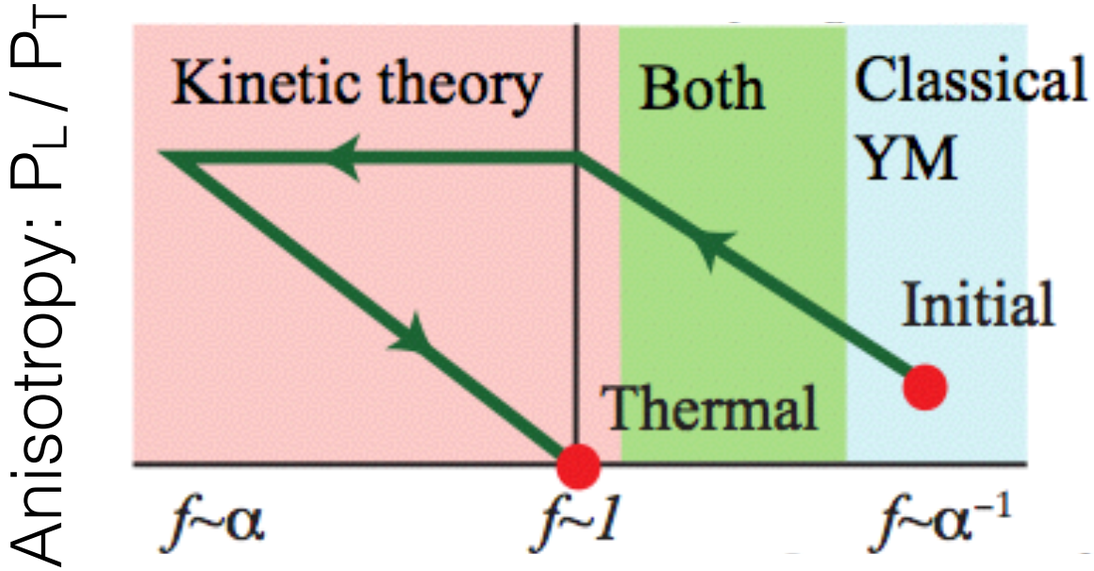

Occupancy: *f*

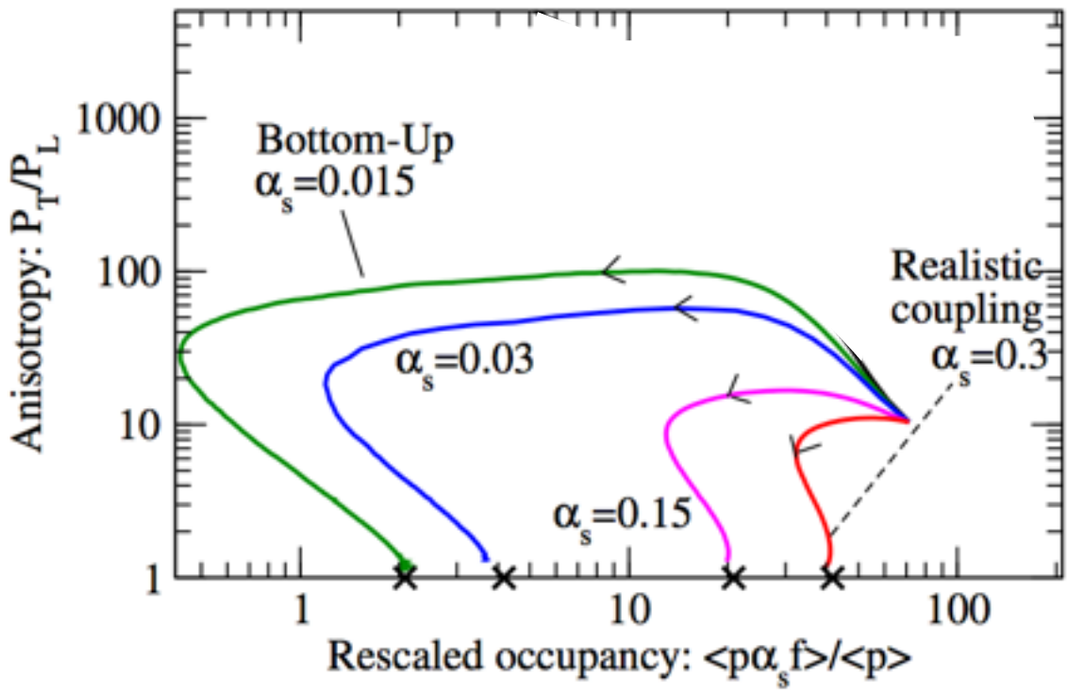

Kurkela, Zhu PRL 115 (2015) 182301

Even though distinctions become less clear
basic mechanism remains the same

Onset of hydrodynamics

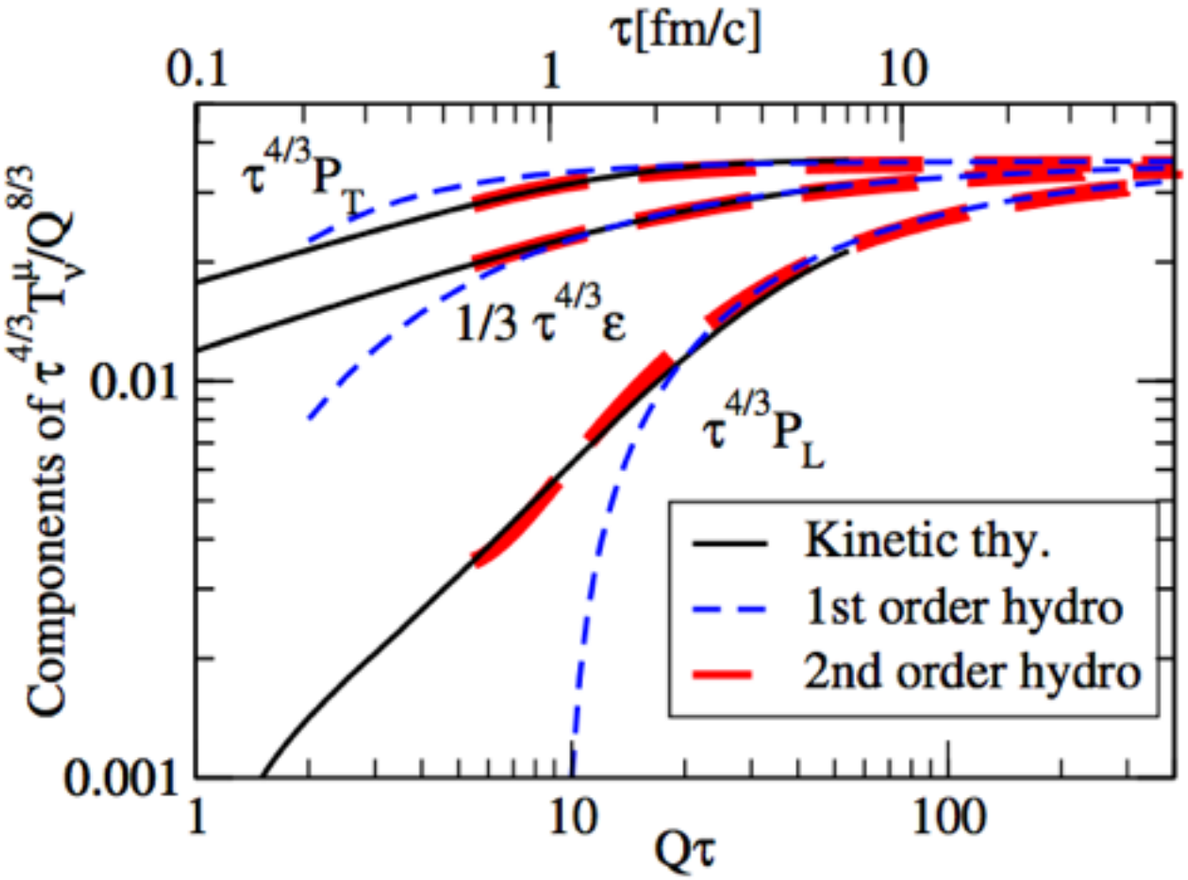

Kurkela, Zhu PRL 115 (2015) 182301

Smooth matching to second order viscous hydrodynamics on a time scale ~1 fm/c

(c.f. talk by Yan Zhu)

Pressure evolution matches for $P_L/P_T \sim 1/5$

-> Equilibration takes much longer than ~1 fm/c for expanding system

Initial conditions for hydro from weak-coupled equilibrium dynamics

(c.f. talk by Aleksas Mazeliauskas)

String tension

Wilson loops

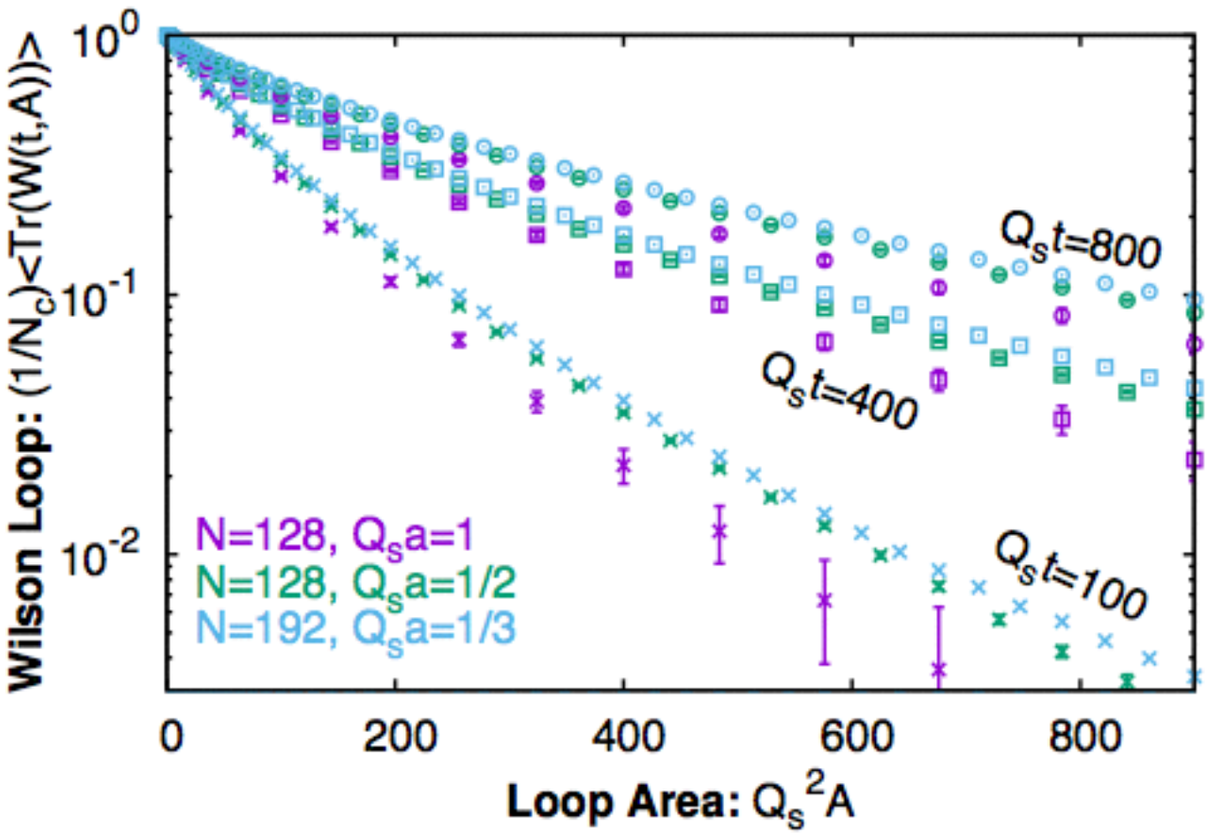

Derivative w.r.t area

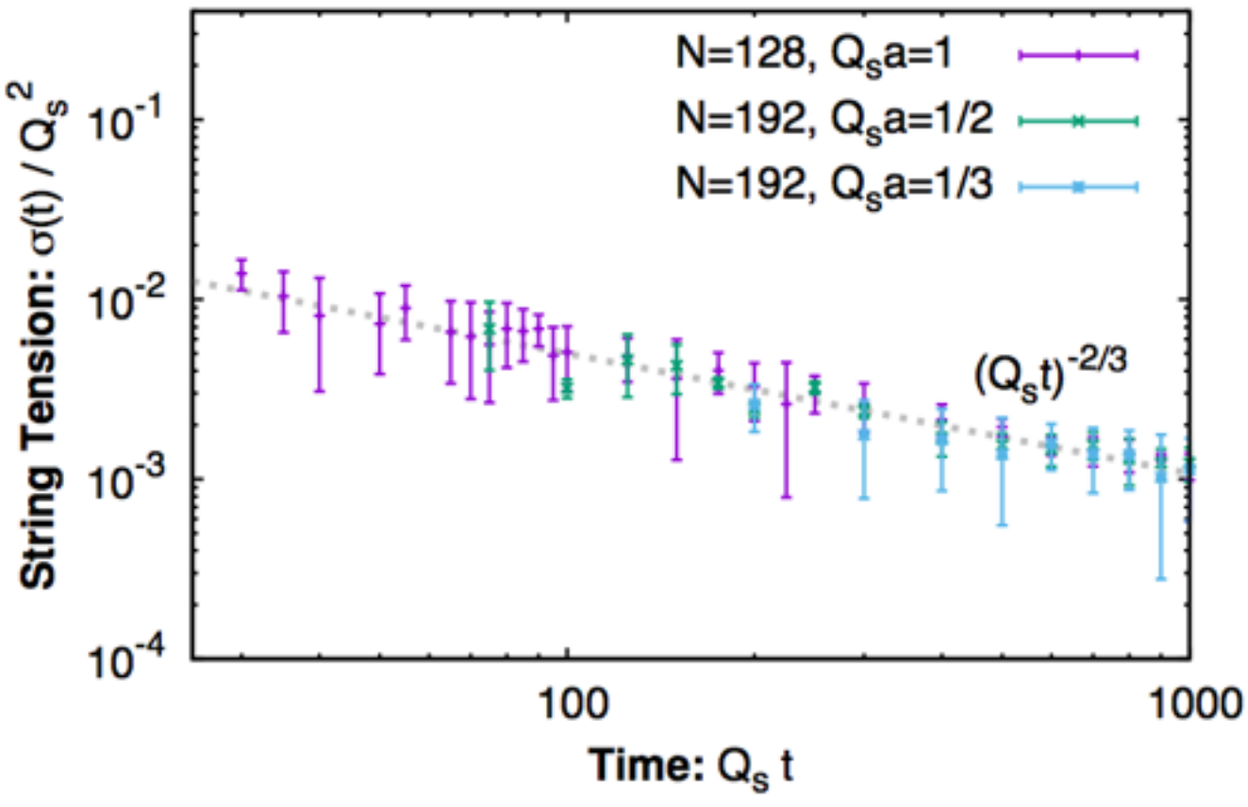

Topology measurement

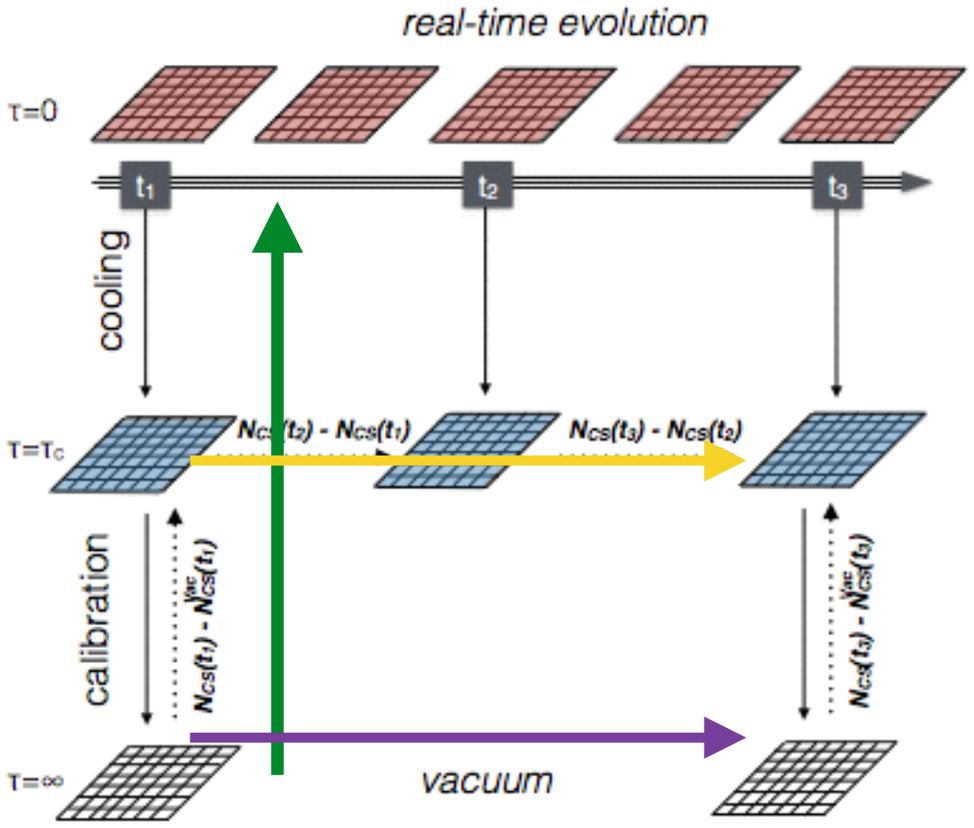

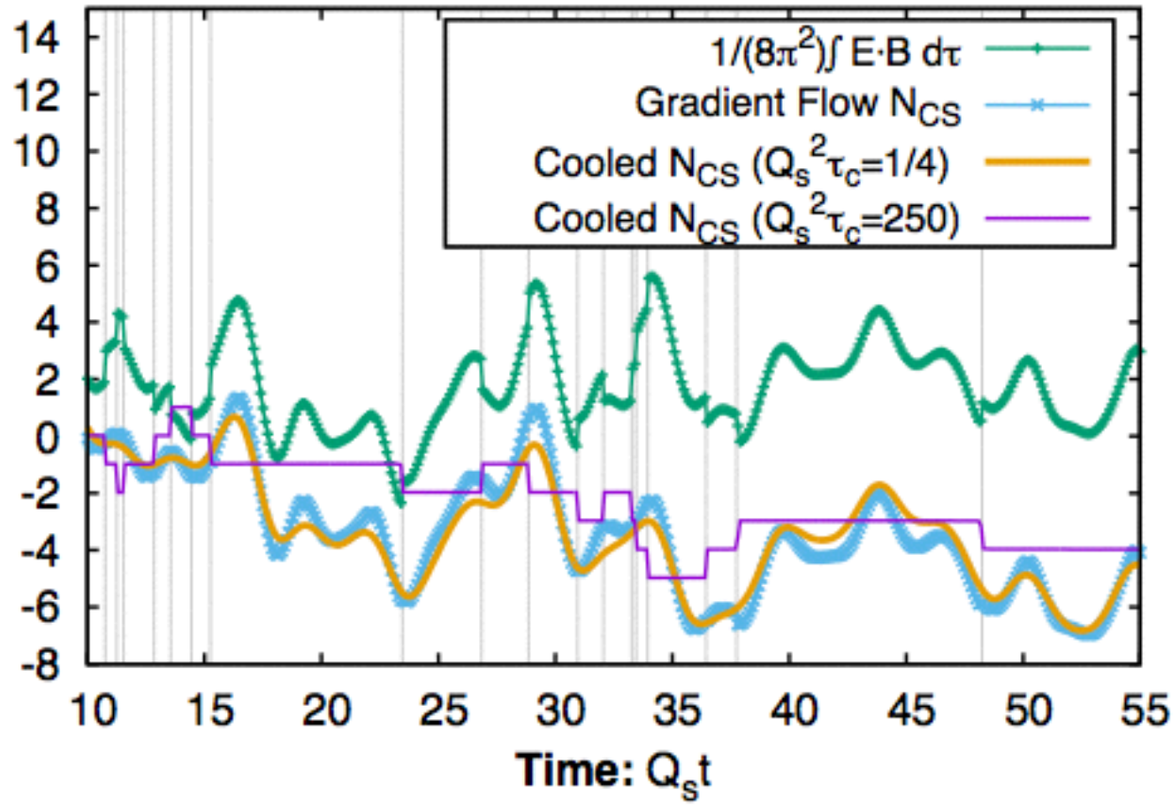

Topology measurement

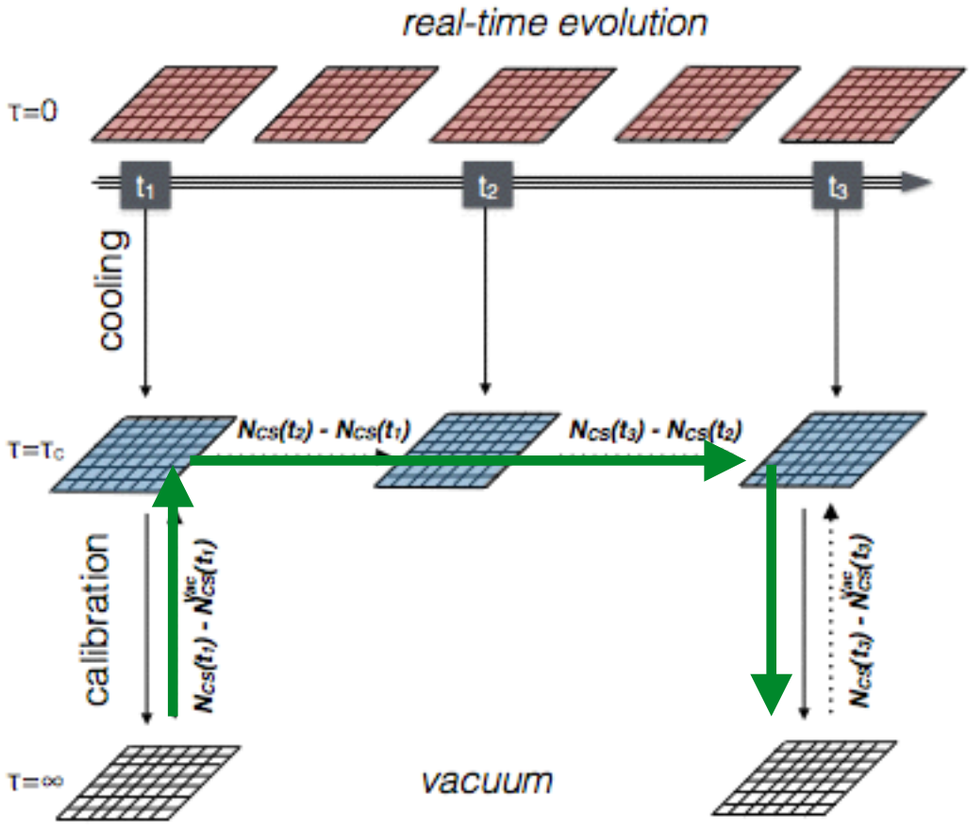

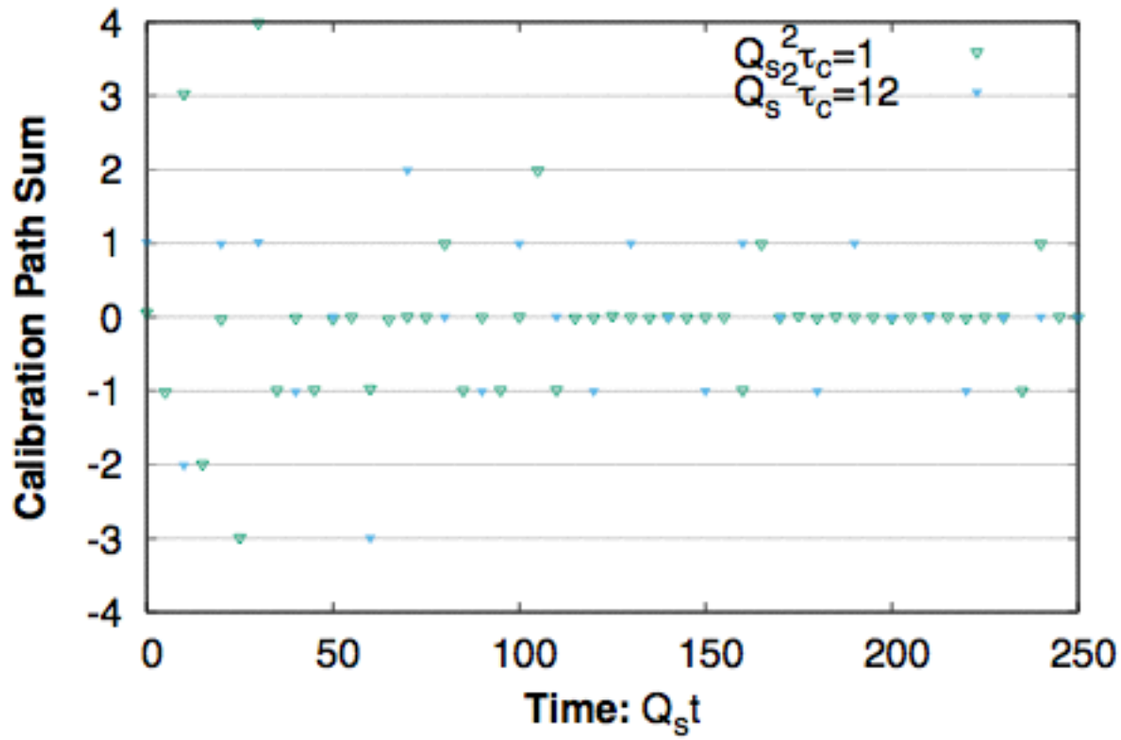

Chern-Simons number Histograms

Generated early (10<Qt<20)

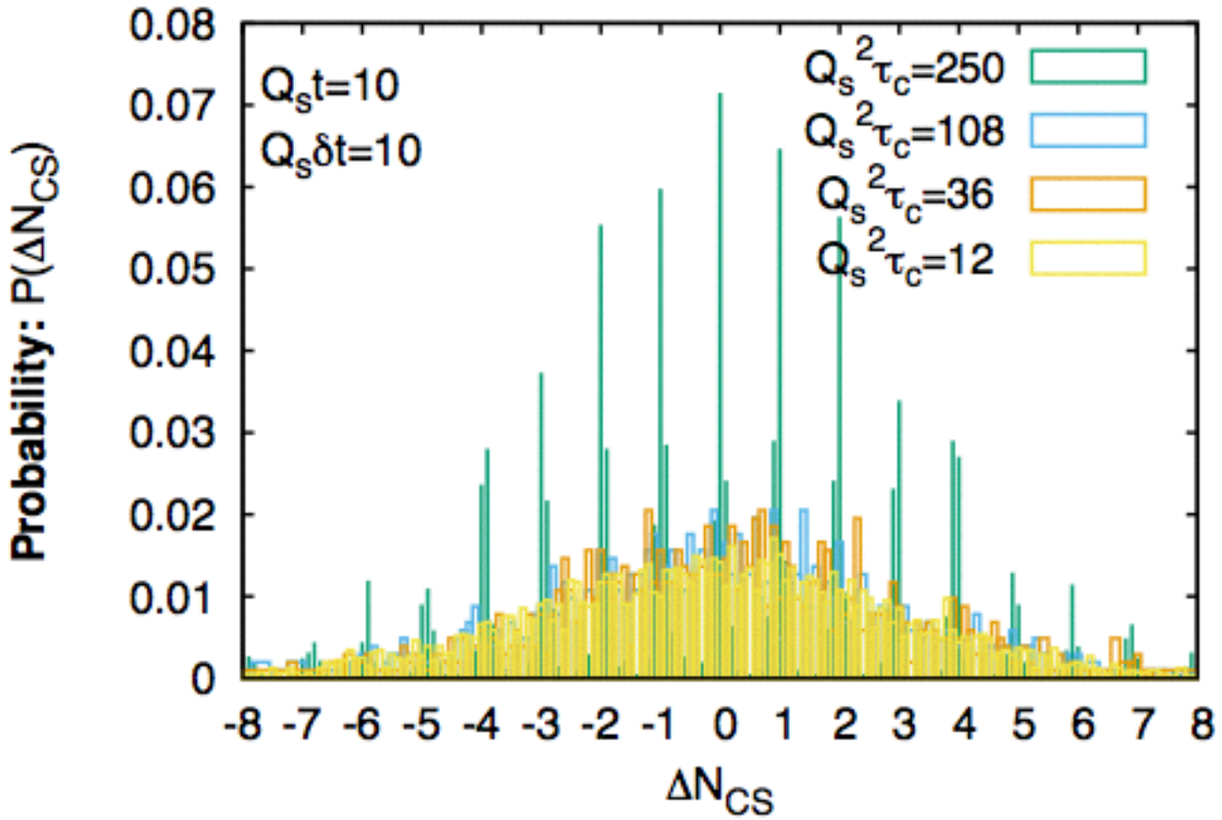

Generated later (50<Qt<60)

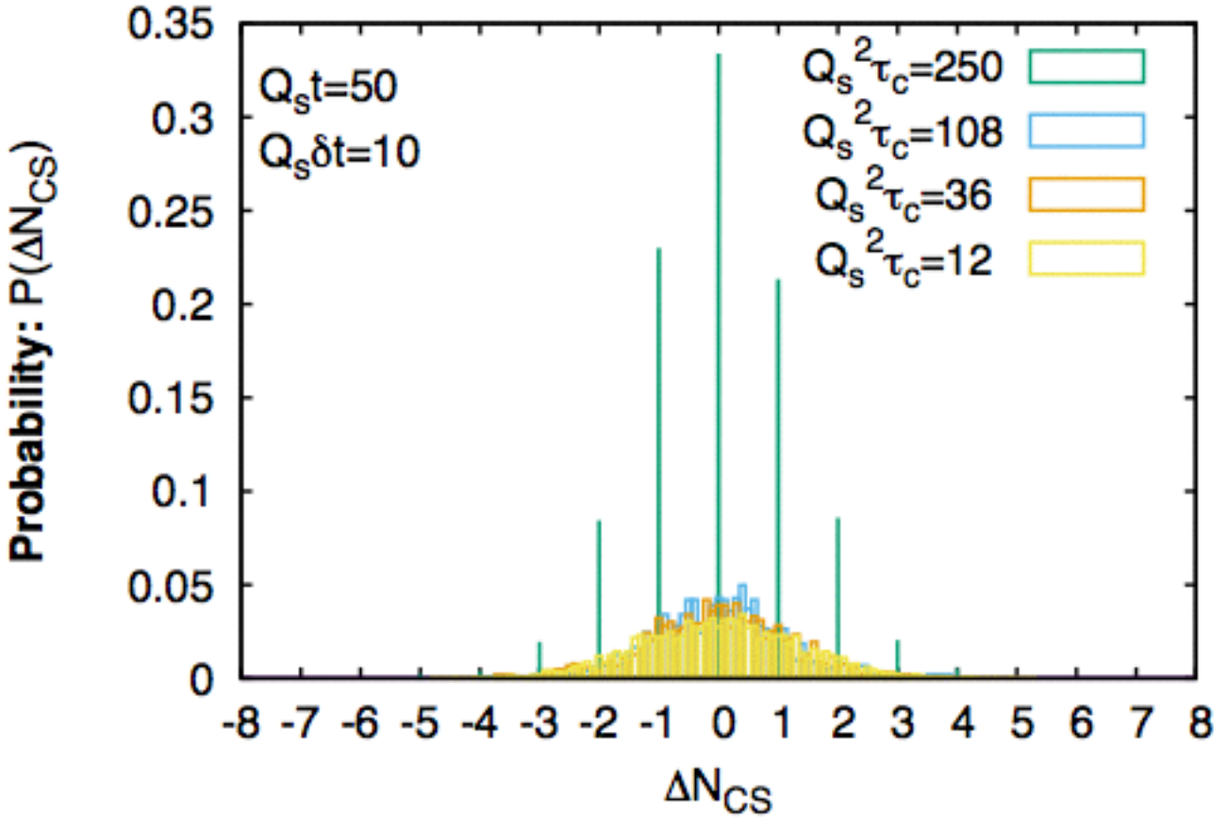

-> Early times dominate generation of axial charge imbalance

Mace, SS, Venugopalan PRD93 (2016) no.7, 074036

Dependence on IC and Cooling depth

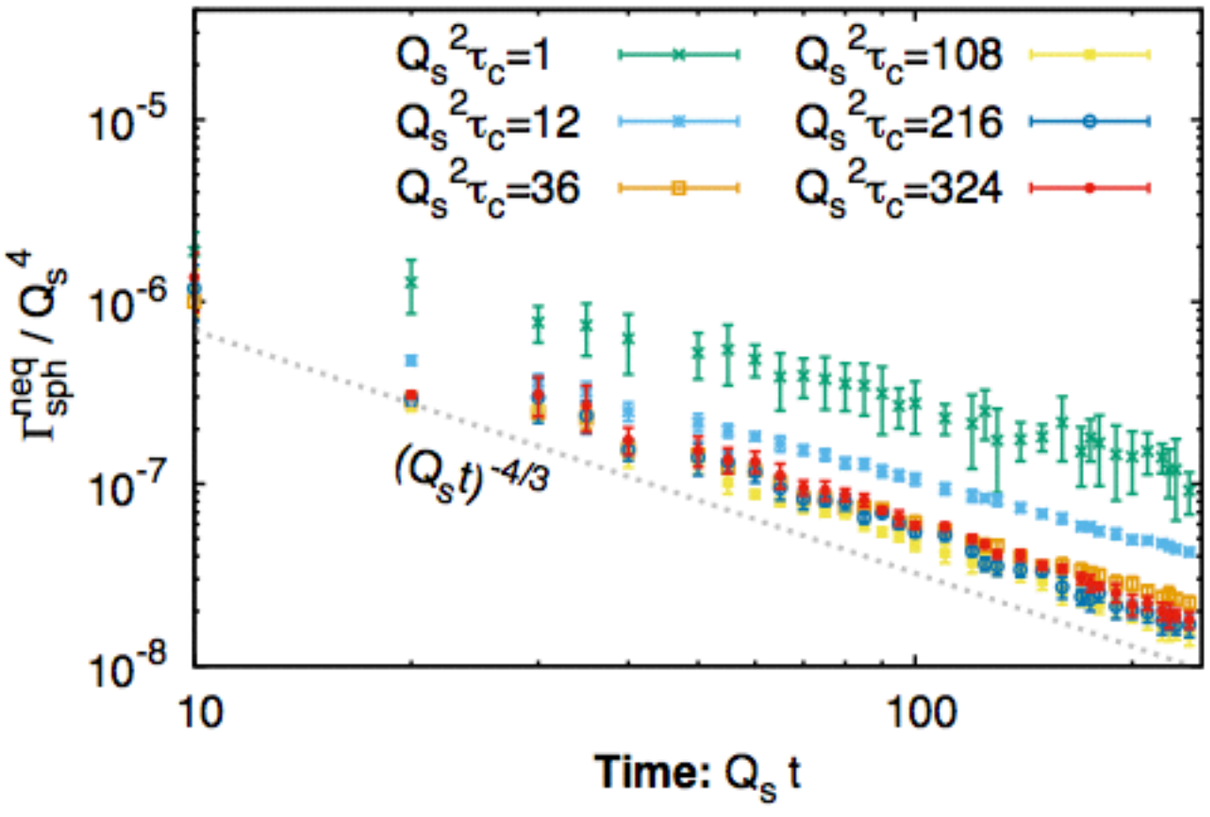

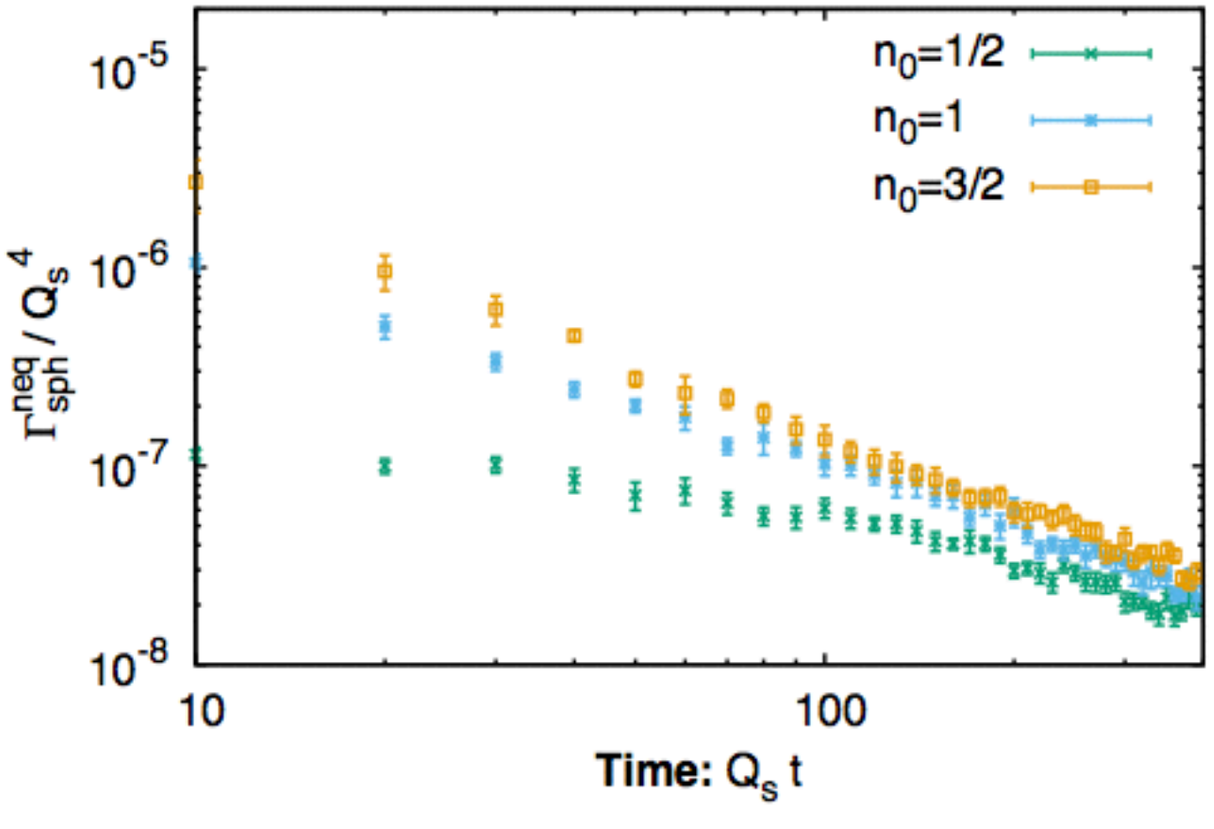

Volume independence